# PHOTOCHEMISTRY OF THE LOWER THERMOSPHERE AND MESOSPHERE

PRESENTED AT THE 1993 ANNUAL CEDAR MEETING

by

D .G. TORR

OPTICAL AERONOMY LABORATORY
CENTER FOR SPACE PLASMA AND AERONOMIC RESEARCH
UNIVERSITY OF ALABAMA IN HUNTSVILLE

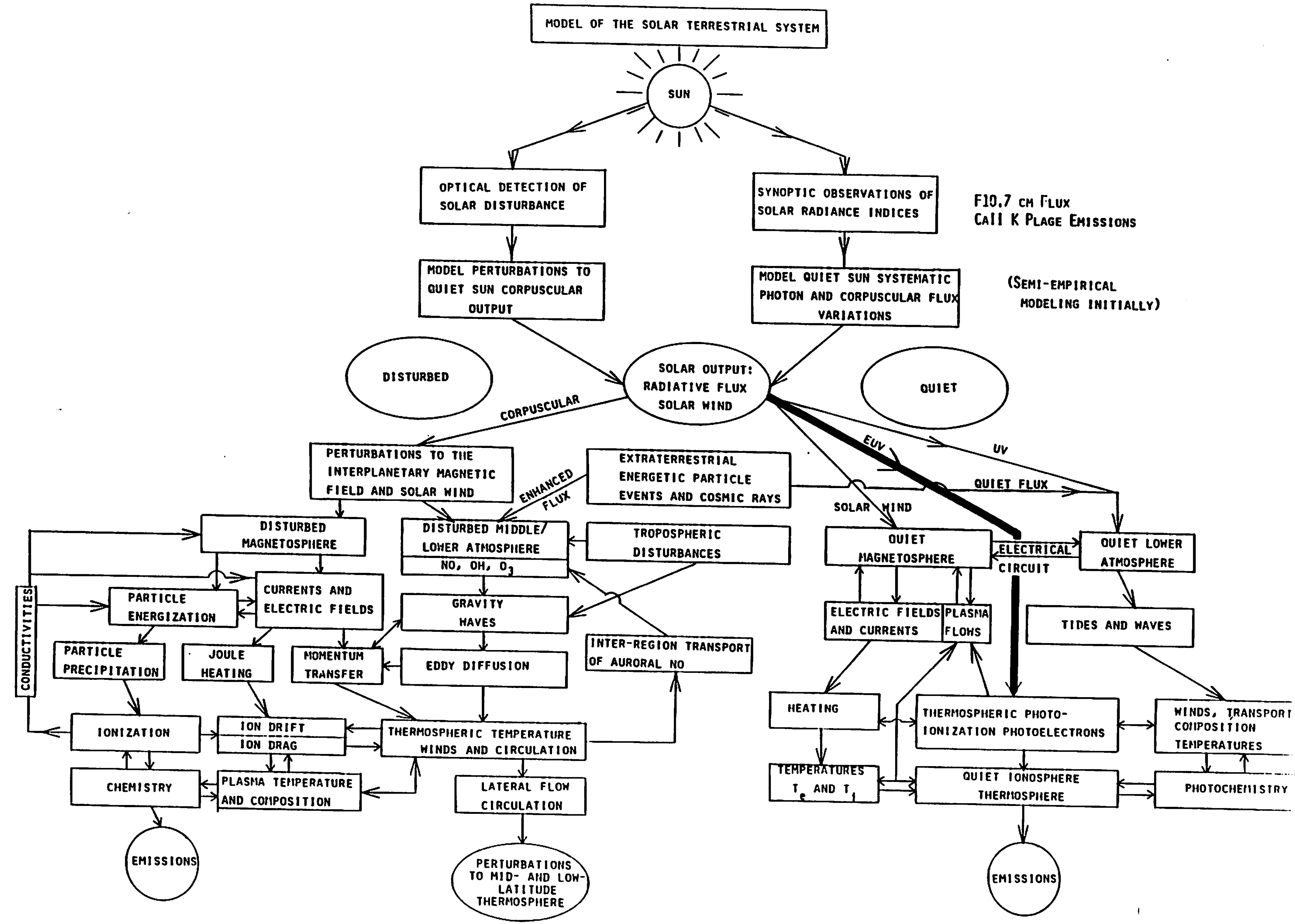
MODEL OF THE SOLAR TERRESTRIAL SYSTEM
SUN
OPTICAL DETECTION OF SOLAR DISTURBANCE
SYNOPTIC OBSERVATIONS OF SOLAR RADIANCE INDICES
F10.7 cm Flux
CaII K Plage Emissions
MODEL PERTURBATIONS TO QUIET SUN CORPUSCULAR OUTPUT
MODEL QUIET SUN SYSTEMATIC PHOTON AND CORPUSCULAR FLUX VARIATIONS
(Semi-empirical modeling initially)
DISTURBED
SOLAR OUTPUT: RADIATIVE FLUX SOLAR WIND
QUIET
CORPUSCULAR
EUV
UV
PERTURBATIONS TO THE INTERPLANETARY MAGNETIC FIELD AND SOLAR WIND
ENHANCED FLUX
EXTRATERRESTRIAL ENERGETIC PARTICLE EVENTS AND COSMIC RAYS
QUIET FLUX
SOLAR WIND
DISTURBED MAGNETOSPHERE
DISTURBED MIDDLE/ LOWER ATMOSPHERE
NO, OH, $O_3$
TROPOSPHERIC DISTURBANCES
QUIET MAGNETOSPHERE
ELECTRICAL CIRCUIT
QUIET LOWER ATMOSPHERE
CONDUCTIVITIES
PARTICLE ENERGIZATION
CURRENTS AND ELECTRIC FIELDS
GRAVITY WAVES
ELECTRIC FIELDS AND CURRENTS
PLASMA FLOWS
TIDES AND WAVES
PARTICLE PRECIPITATION
JOULE HEATING
MOMENTUM TRANSFER
EDDY DIFFUSION
INTER-REGION TRANSPORT OF AURORAL NO
HEATING
THERMOSPHERIC PHOTO-IONIZATION PHOTOELECTRONS
WINDS, TRANSPORT, COMPOSITION TEMPERATURES
IONIZATION
ION DRIFT
ION DRAG
THERMOSPHERIC TEMPERATURE WINDS AND CIRCULATION
TEMPERATURES $T_e$ AND $T_i$
QUIET IONOSPHERE THERMOSPHERE
PHOTOCHEMISTRY
CHEMISTRY
PLASMA TEMPERATURE AND COMPOSITION
LATERAL FLOW CIRCULATION
EMISSIONS
PERTURBATIONS TO MID- AND LOW-LATITUDE THERMOSPHERE
EMISSIONS

SCIENCE OBJECTIVES: THE COUPLED IONOSPHERE THERMOSPHERE MESOSPHERE SYSTEM

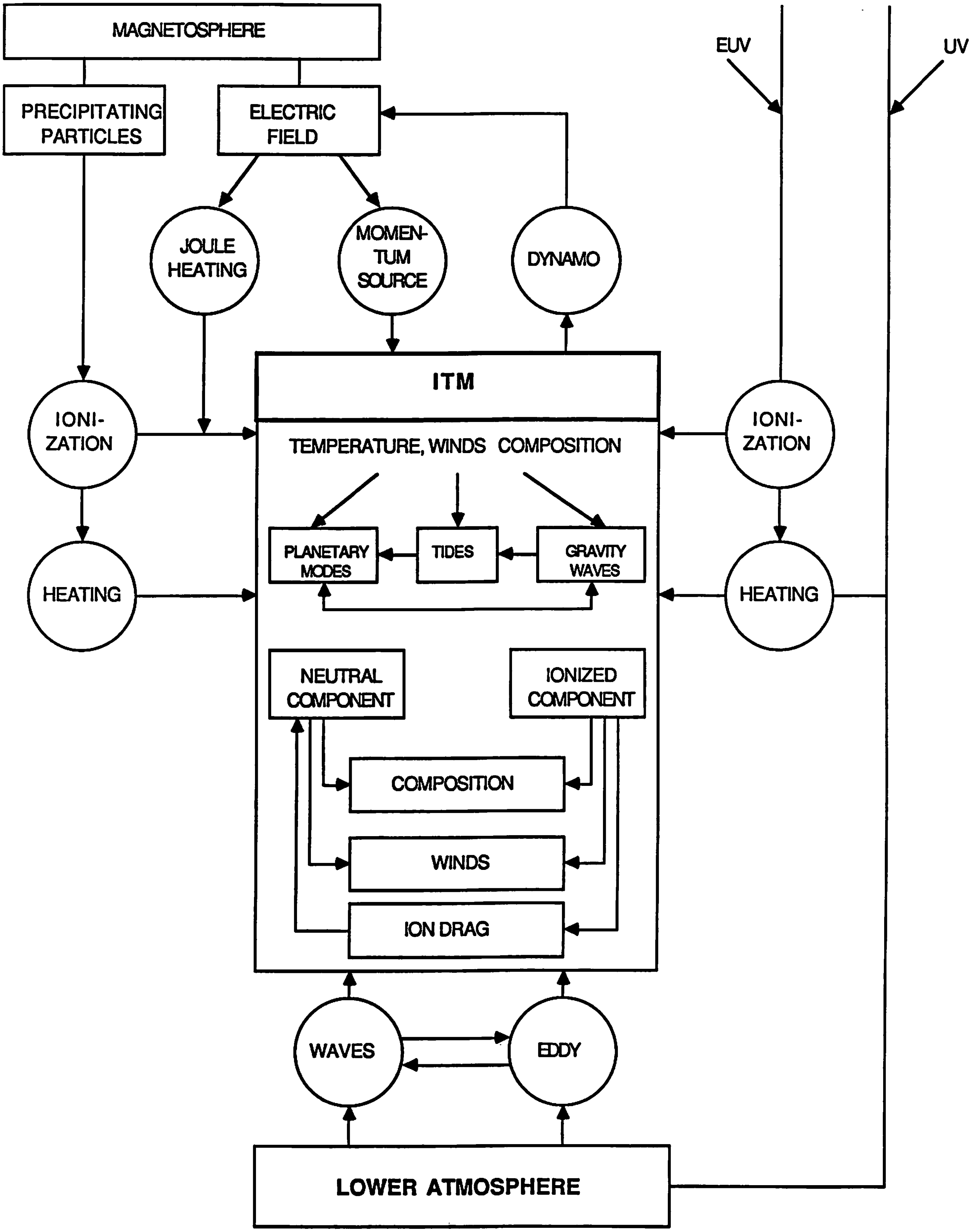

# BASIC THERMOSPHERIC PHOTOCHEMISTRY

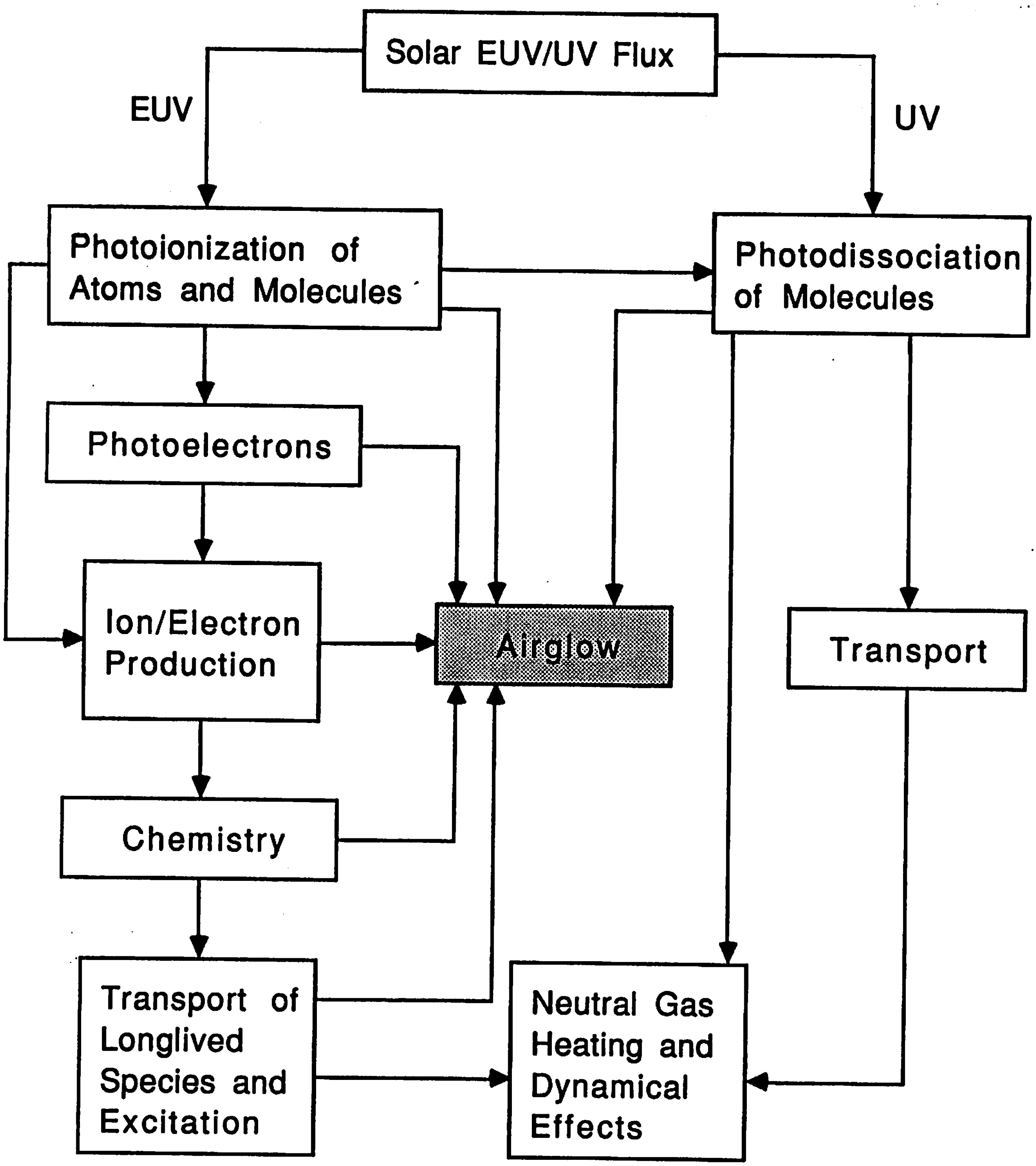

## Temperature Structure of the Atmosphere

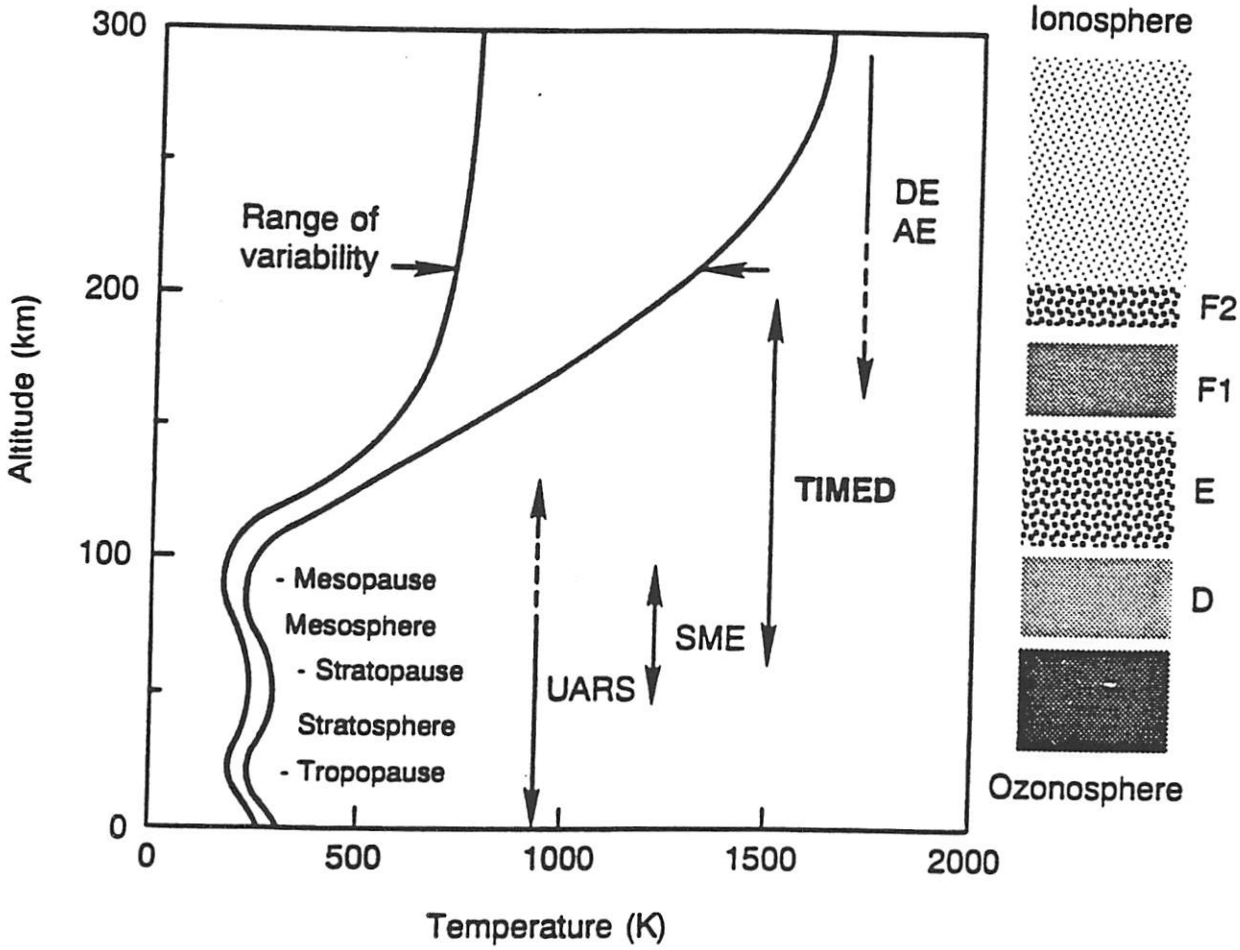


Temperature structure of the atmosphere and nomenclature for those regions defined by the temperature structure. The TIMED Mission will provide the first comprehensive experimental investigation of the critical transition region characterized by the most rapidly changing lapse rates in the Earth's atmosphere. Regions mentioned by other NASA missions are indicated.

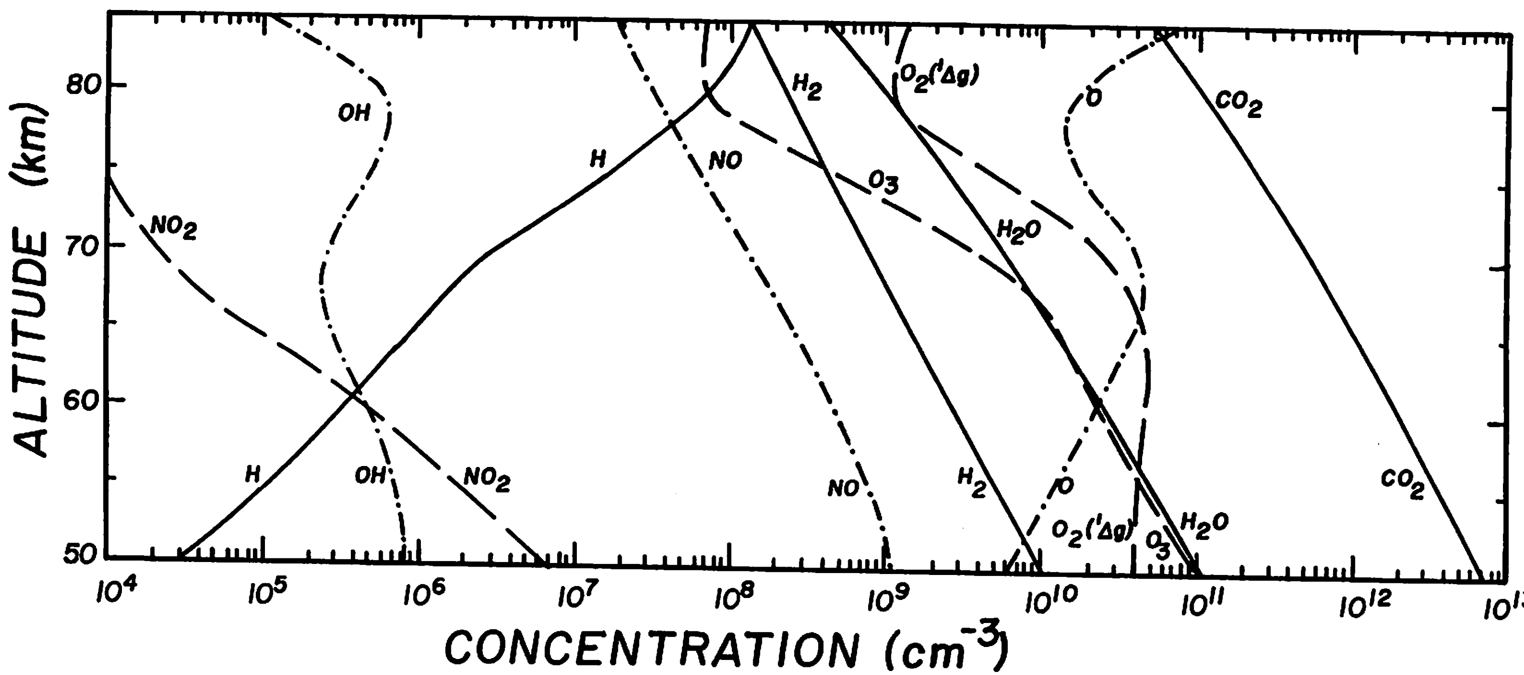


Mesospheric Constituents (Wisemburg and Kockarts, 1980)

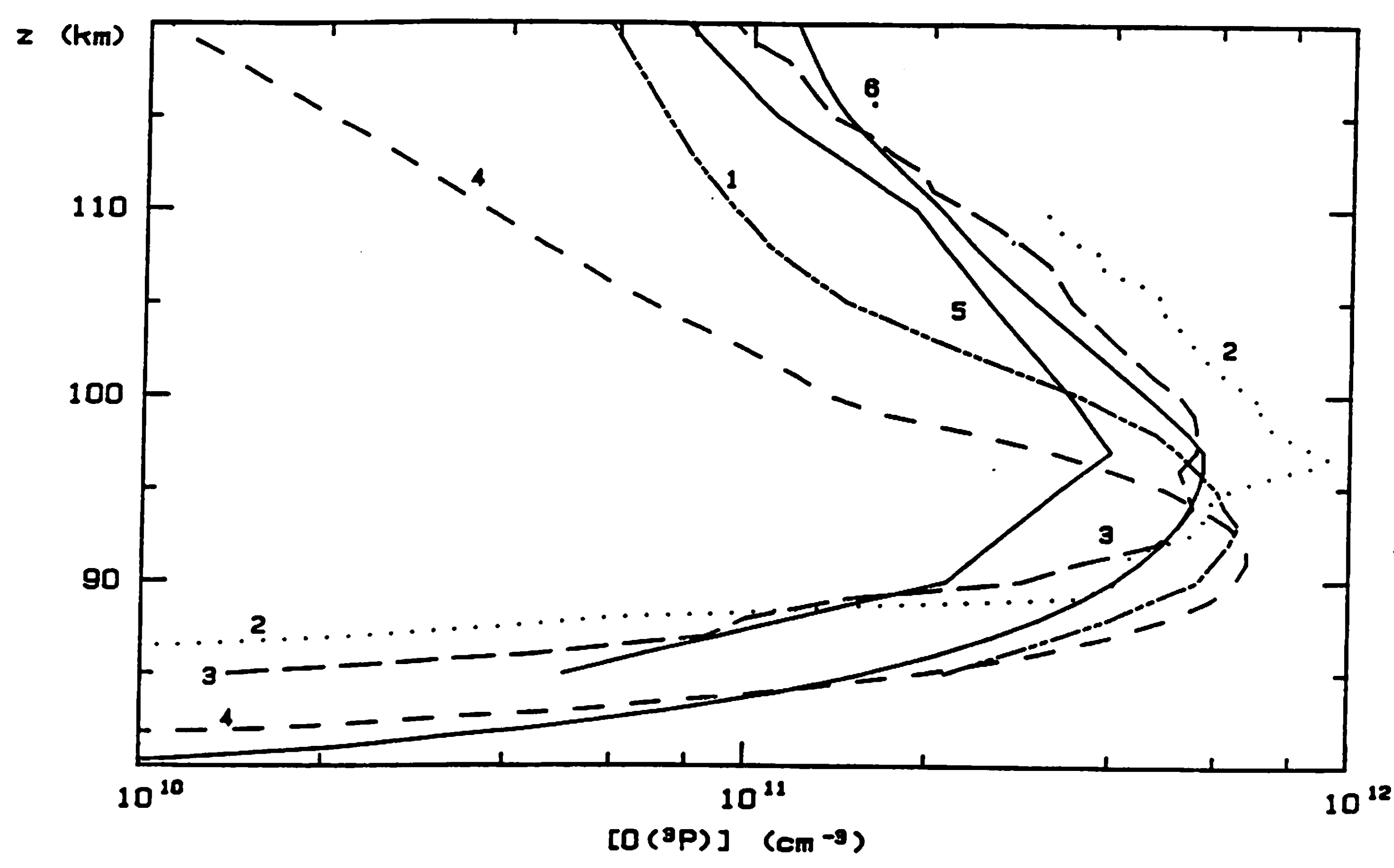


FIG. 10. NIGHTTIME ATOMIC OXYGEN PROFILE.
Curve 1: Trinks *et al.* (1978). Curve 2: Thomas *et al.* (1979). Curve 3: Thomas (1981). Curve 4: Rodrigo *et al.* (1981). Curve 5: Hedin (1983). Curve 6: This model.

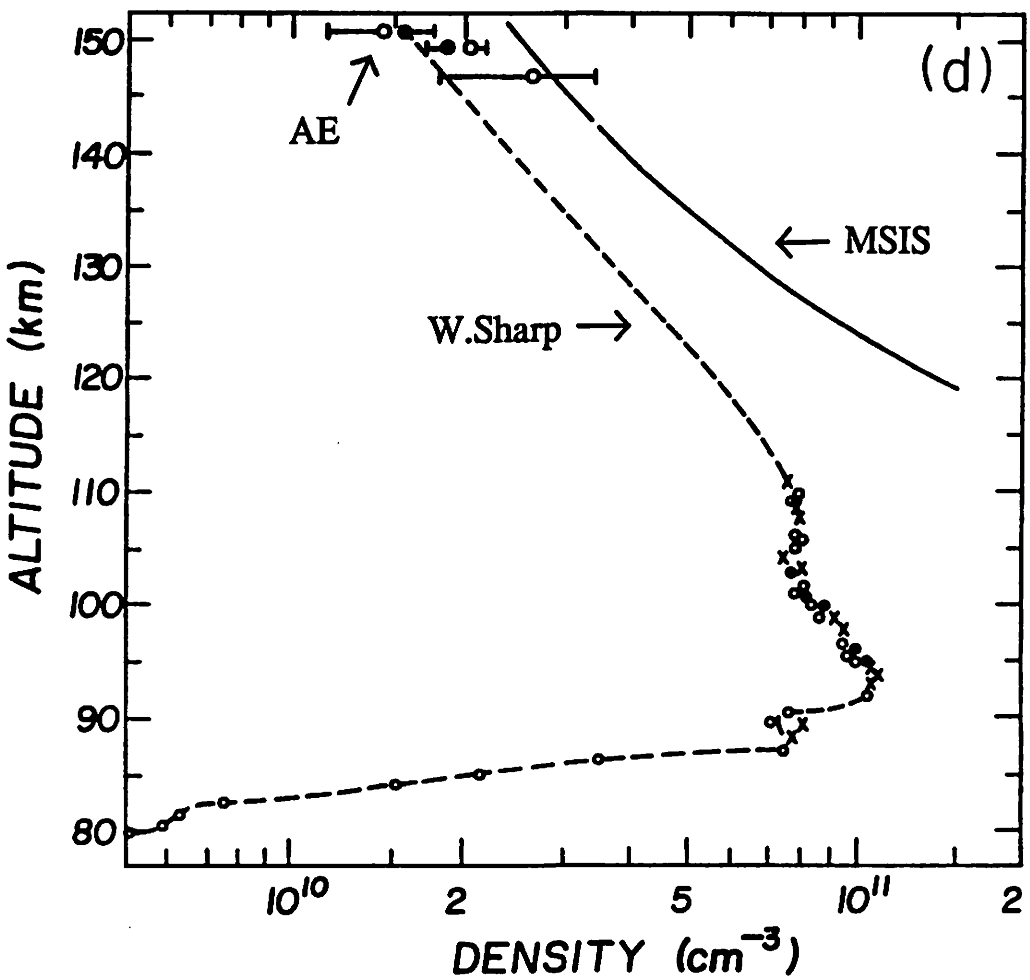


ATOMIC OXYGEN

# Solar

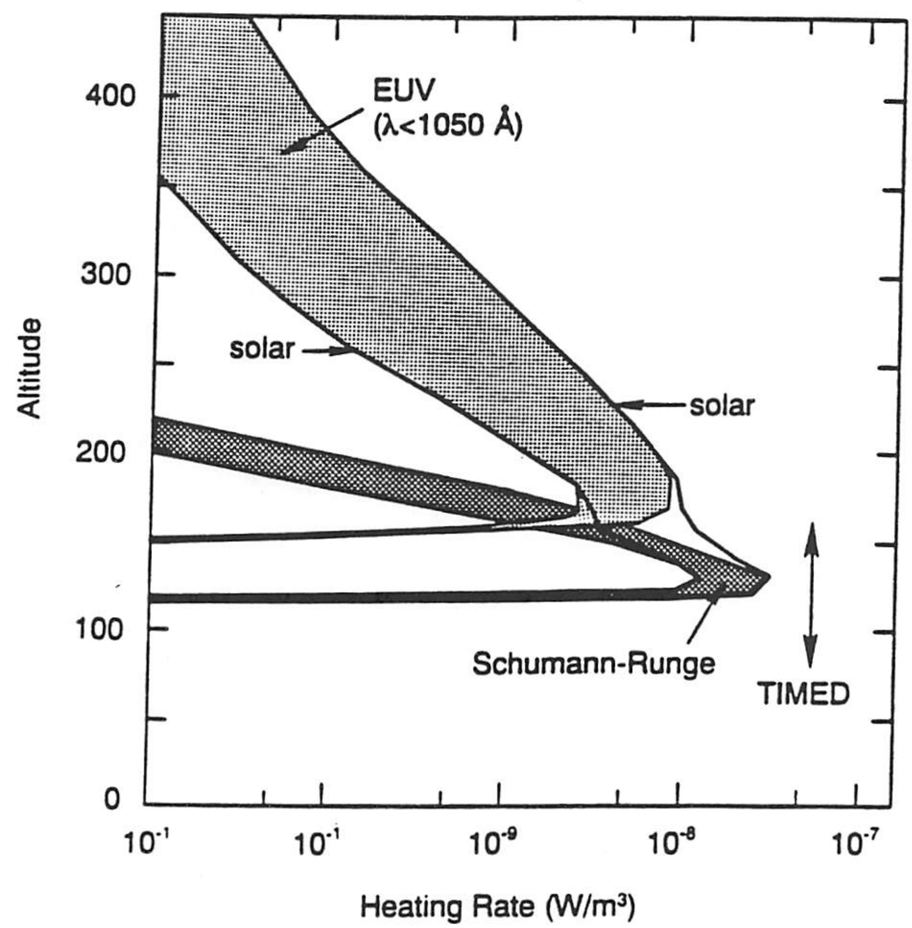


Altitudinal profiles of heating rates due to solar EUV and UV absorption. The shaded regions indicate the range of variations with solar activity. The TIMED Mission investigates the region of maximum energy deposition.

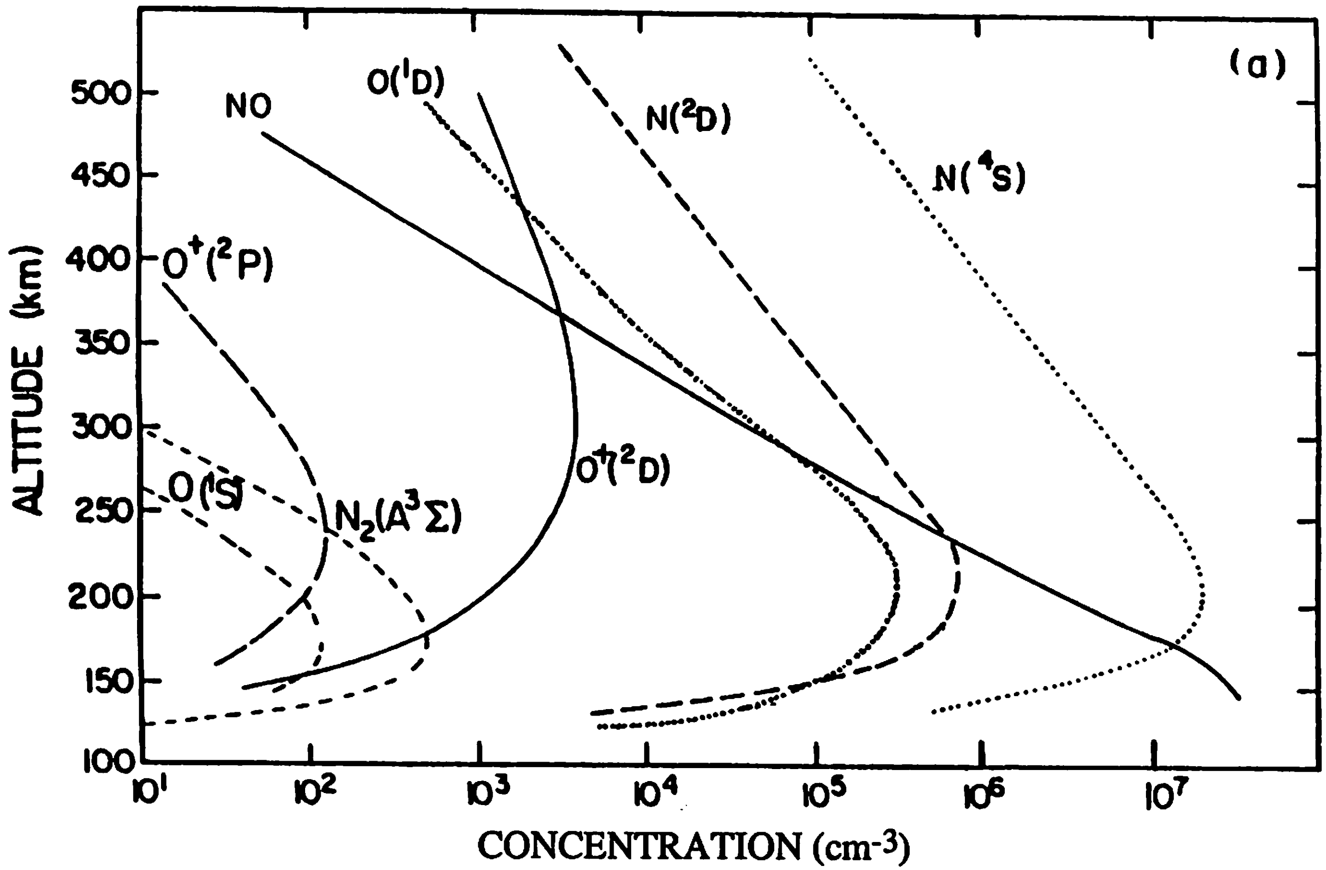
(a)
NO
O(1D)
N(2D)
N(4S)
O+(2P)
O+(2D)
O(1S)
N2(A3Σ)
ALTITUDE (km)
500
450
400
350
300
250
200
150
100
10¹
10²
10³
10⁴
10⁵
10⁶
10⁷
CONCENTRATION (cm-3)

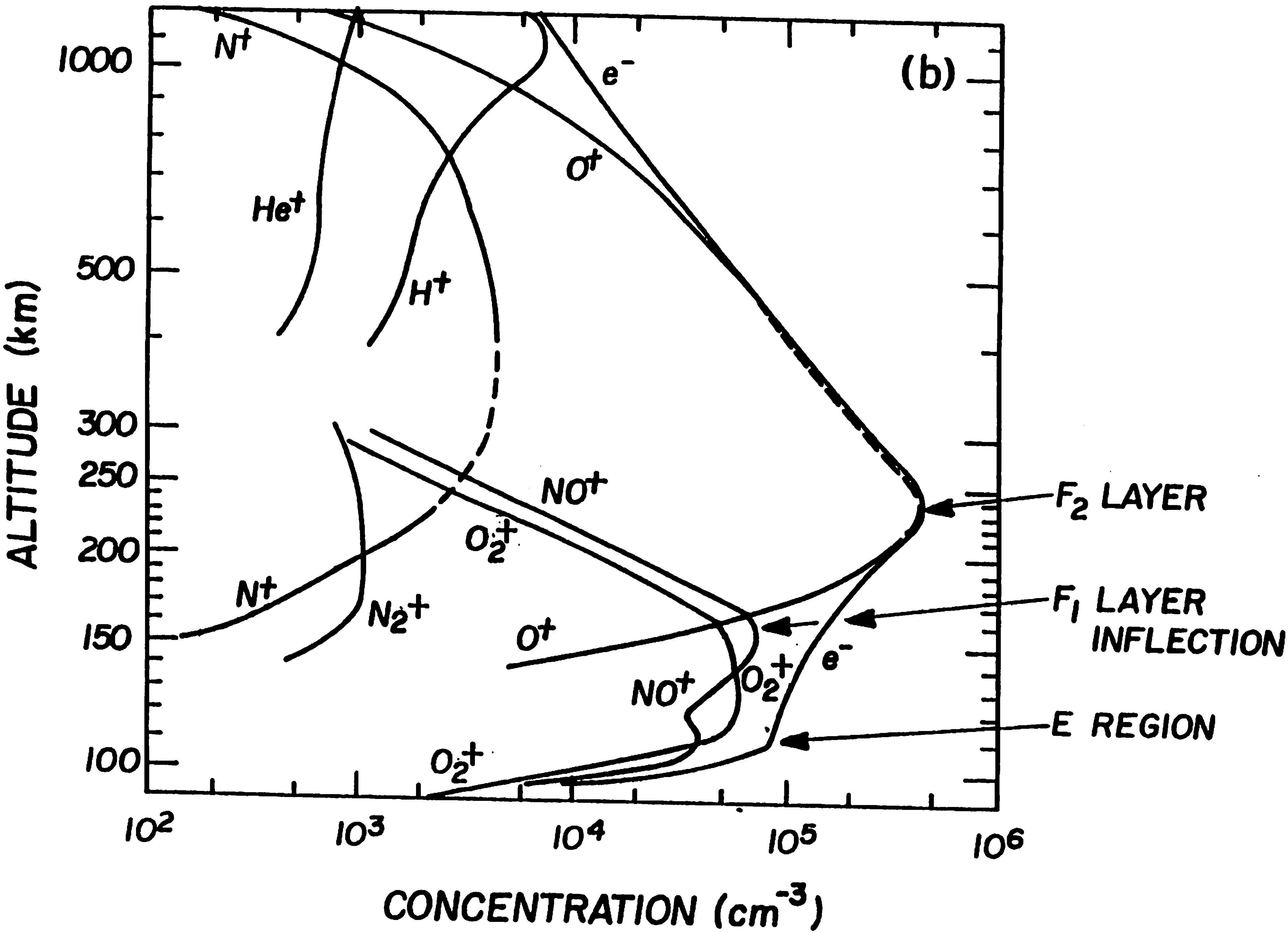

(b)
ALTITUDE (km)
1000
500
300
250
200
150
100
$N^+$
$He^+$
$H^+$
$O^+$
$e^-$
$NO^+$
$O_2^+$
$N_2^+$
F2 LAYER
F1 LAYER INFLECTION
E REGION
$10^2$
$10^3$
$10^4$
$10^5$
$10^6$
CONCENTRATION ($cm^{-3}$)

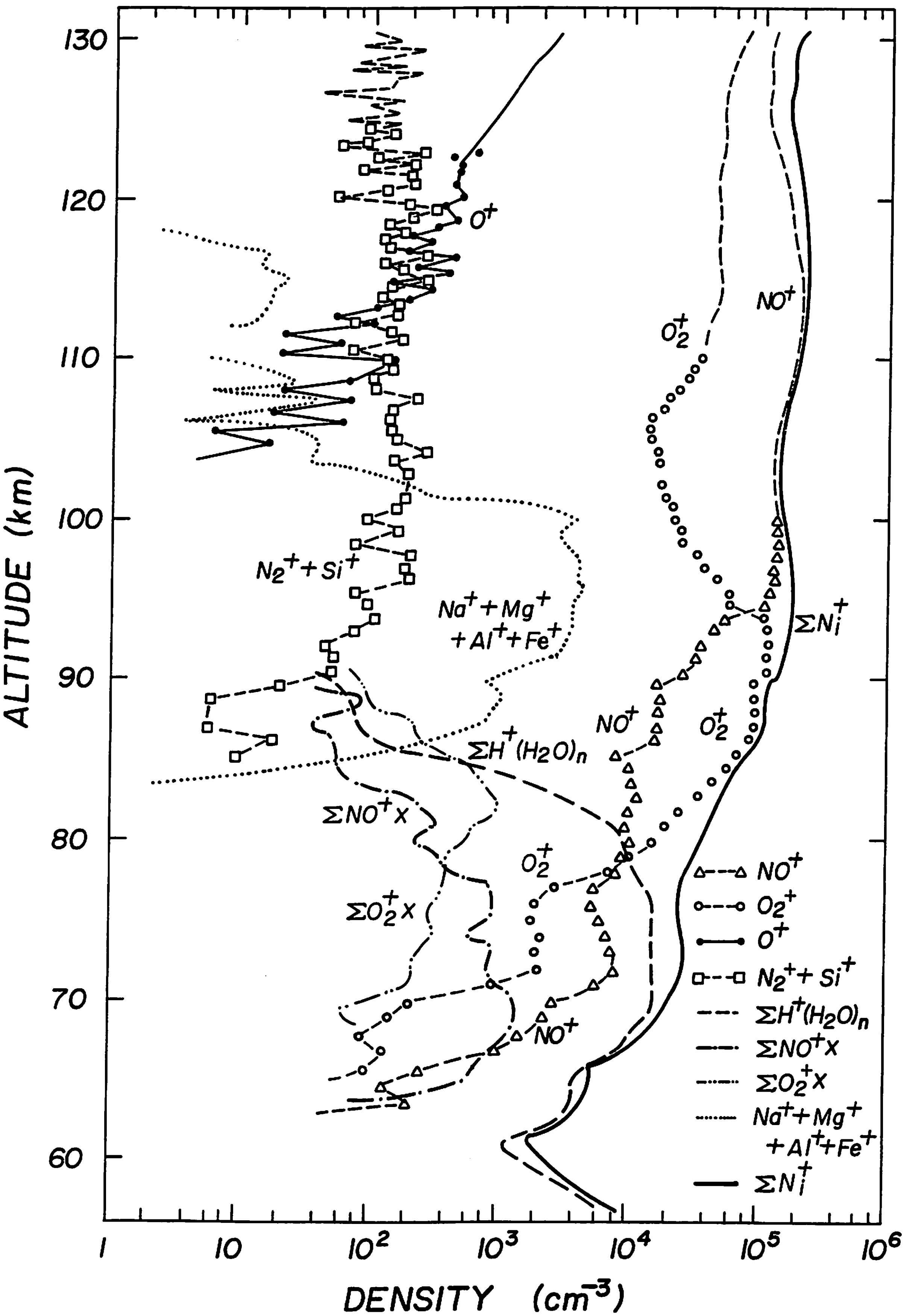


Kopp and Hermann (1982)

# WHY IS PHOTOCHEMISTRY IMPORTANT?

**COMPOSITION AND TEMPERATURE:**

PHOTOCHEMISTRY PLAYS A FUNDAMENTAL ROLE IN CONTROLLING SPECIES ABUNDANCE AND THERMAL STRUCTURE, (ENERGETICS) AND IS AN IMPORTANT ENERGY SOURCE THAT DRIVES DYNAMICS.

**PHOTOCHEMICAL - DYNAMICAL COUPLING:**

VARIATIONS IN CHEMICAL COMPOSITION RAPIDLY INFLUENCE THE THERMAL STRUCTURE AND DYNAMICS OF THE MESOSPHERE AND LOWER THERMOSPHERE, AND VICE-VERSA

**ENERGETICS:**

PHOTOCHEMICALLY PRODUCED MINOR CONSTITUENTS PLAY IMPORTANT ROLES IN CONTROLLING ENERGETICS

CONSTITUENTS ABSORB SOLAR AND CORPUSCULAR ENERGY, RESULTING IN EXCITATION, DISSOCIATION OR IONIZATION WHICH CAN BE COLLISIONALLY TRANSFERRED EITHER LOCALLY OR NON LOCALLY TO THE SURROUNDING ATMOSPHERE RESULTING IN HEATING.

PHOTOCHEMISTRY PLAYS A CRITICAL ROLE IN DETERMINING THE PARTITIONING AND REDISTRIBUTION OF THE ABSORBED ENERGY, AND HENCE THE EFFICIENCY OF CONVERSION TO HEAT.

RADIATIVE LOSS IS THE PRIMARY COOLING PROCESS AND THIS TOO IS CONTROLLED BY PHOTOCHEMICAL INTERACTIONS.

# WHY IS PHOTOCHEMISTRY IMPORTANT?
# (Continued)

**GENERATES OBSERVABLES:**

INVERSE PHOTOCHEMICAL MODELING OF MEASURED AIRGLOW, AURORAL EMISSIONS AND ELECTRON DENSITY PROVIDES A POWERFUL APPROACH FOR DETERMINING MANY GEOPHYSICAL PARAMETERS *E.G.* COMPOSITION, TEMPERATURE AND ENERGY INPUTS.

## ADVANTAGES OF A QUANTITATIVE UNDERSTANDING OF PHOTOCHEMISTRY

- PHOTOCHEMISTRY IS FUNDAMENTAL TO ALL MLTI MODELING.

- PROVIDES A POWERFUL MEANS FOR RETRIEVING KEY PARAMETERS FROM BOTH ORBITAL AND GROUNDBASED MEASUREMENTS OF PLASMA DENSITIES AND RADIATION FIELDS.

- **KNOWLEDGE OF NEUTRAL (AND ION) COMPOSITION, TEMPERATURE AND INPUT ENERGY FLUXES WILL PROVIDE CRITICAL TESTS OF GLOBAL MODELS.**

  – *E.G.* THE TIE-GCM REQUIRES ENERGY INPUTS AND PROVIDES COMPOSITION AND TEMPERATURE AS OUTPUT.

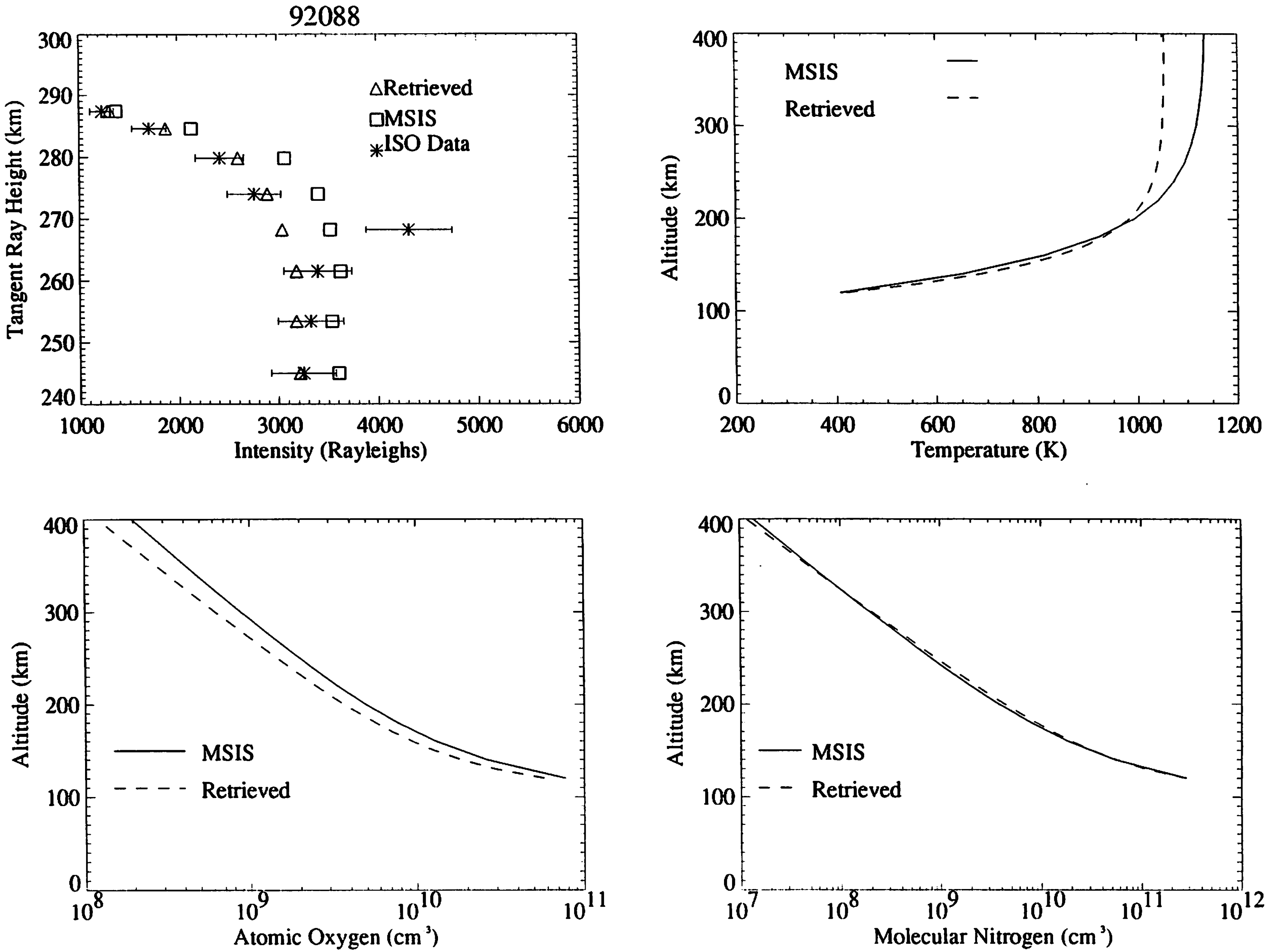
92088
Tangent Ray Height (km)
Intensity (Rayleighs)
Retrieved
MSIS
ISO Data
Altitude (km)
Temperature (K)
MSIS
Retrieved
Altitude (km)
Atomic Oxygen (cm⁻³)
MSIS
Retrieved
Altitude (km)
Molecular Nitrogen (cm⁻³)
MSIS
Retrieved

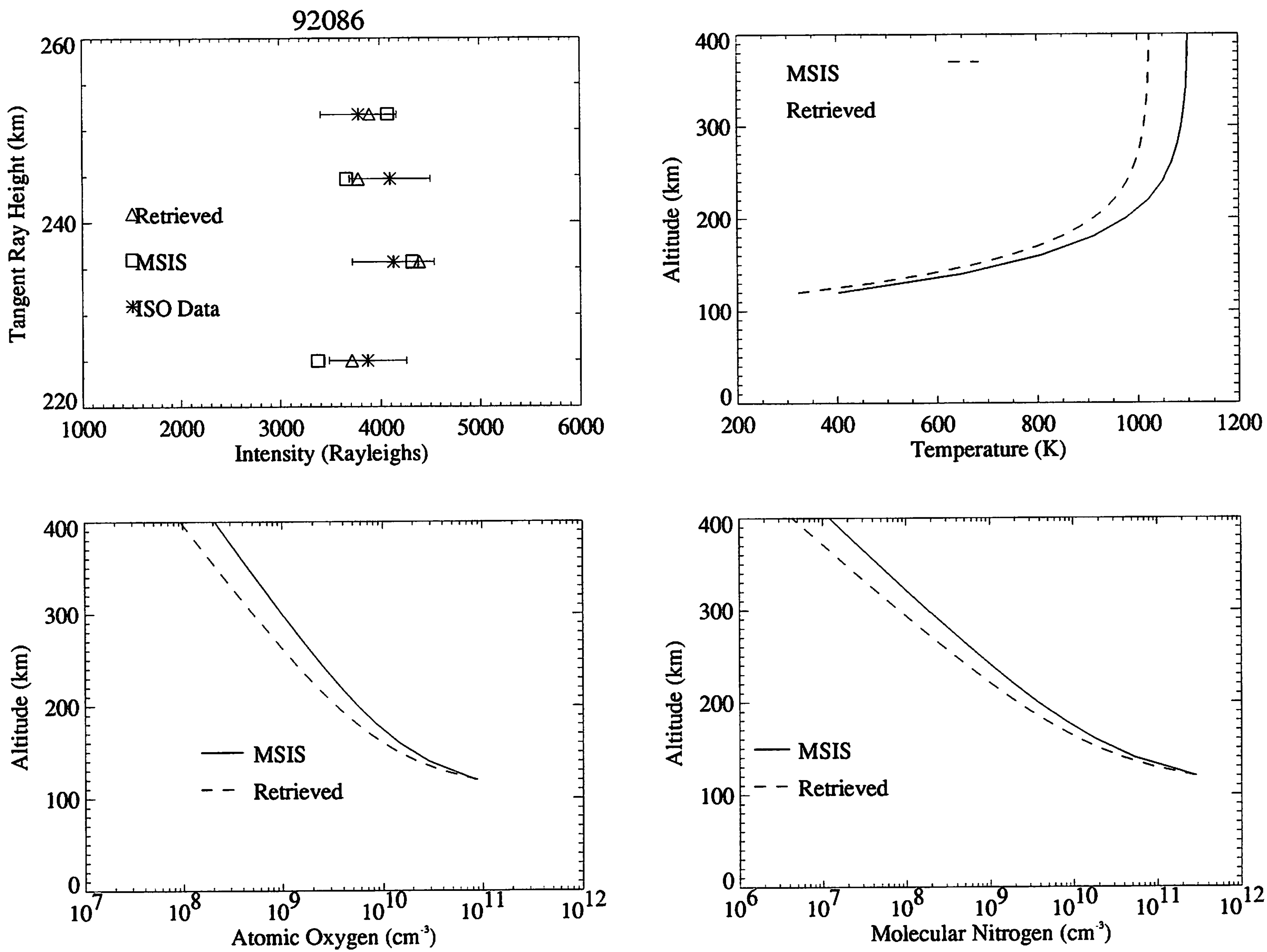

92086
Tangent Ray Height (km)
260
240
220
Retrieved
MSIS
ISO Data
1000
2000
3000
4000
5000
6000
Intensity (Rayleighs)
Altitude (km)
400
300
200
100
0
MSIS
Retrieved
200
400
600
800
1000
1200
Temperature (K)
Altitude (km)
MSIS
Retrieved
$10^7$
$10^8$
$10^9$
$10^{10}$
$10^{11}$
$10^{12}$
Atomic Oxygen ($cm^{-3}$)
Altitude (km)
MSIS
Retrieved
$10^6$
$10^7$
$10^8$
$10^9$
$10^{10}$
$10^{11}$
$10^{12}$
Molecular Nitrogen ($cm^{-3}$)

# STATUS OF PHOTOCHEMICAL UNDERSTANDING

**UPPER THERMOSPHERE:**

- GOOD QUANTITATIVE UNDERSTANDING.

**LOWER THERMOSPHERE:**

- MUCH IN COMMON WITH UPPER THERMOSPHERE - BUT UNPROVEN UNDERSTANDING.

**MESOSPHERE:**

- RELATIVELY GOOD CONCEPTUAL UNDERSTANDING.
- POOR QUANTITATIVE UNDERSTANDING.

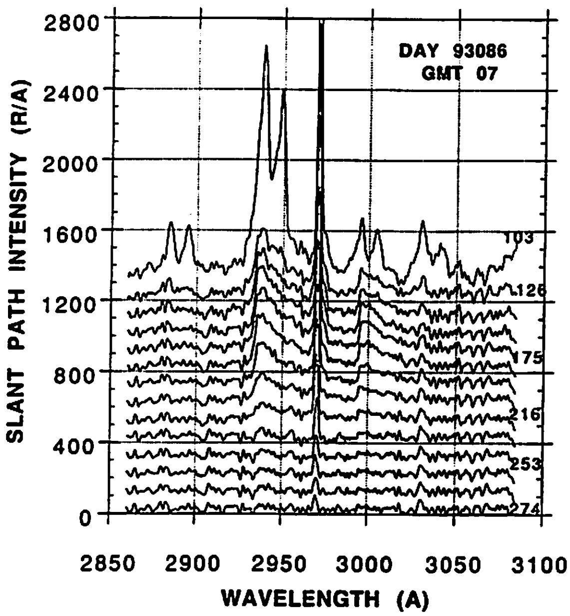


## Conclusions

The ISO has obtained the first broadband spectra of the thermospheric dayglow emissions, providing a database with considerable potential for constraining photochemical models. The agreement between measurement and model for the 12 major dayglow features shown in Figures 3 and 4 is surprisingly good (better than a factor of 2). There are, of course, many details and subtleties that must be studied, and for which this multiparameter database can provide substantial constraints. We conclude that the basic thermospheric photochemistry established on the basis of the Atmosphere Explorer database explains a large number of thermospheric

Fig. 2. Example of the spectra obtained at different tangent ray heights in the course of the roll maneuver. While the absolute scale is the same for each, the various spectra have offsets added in order to display the data.

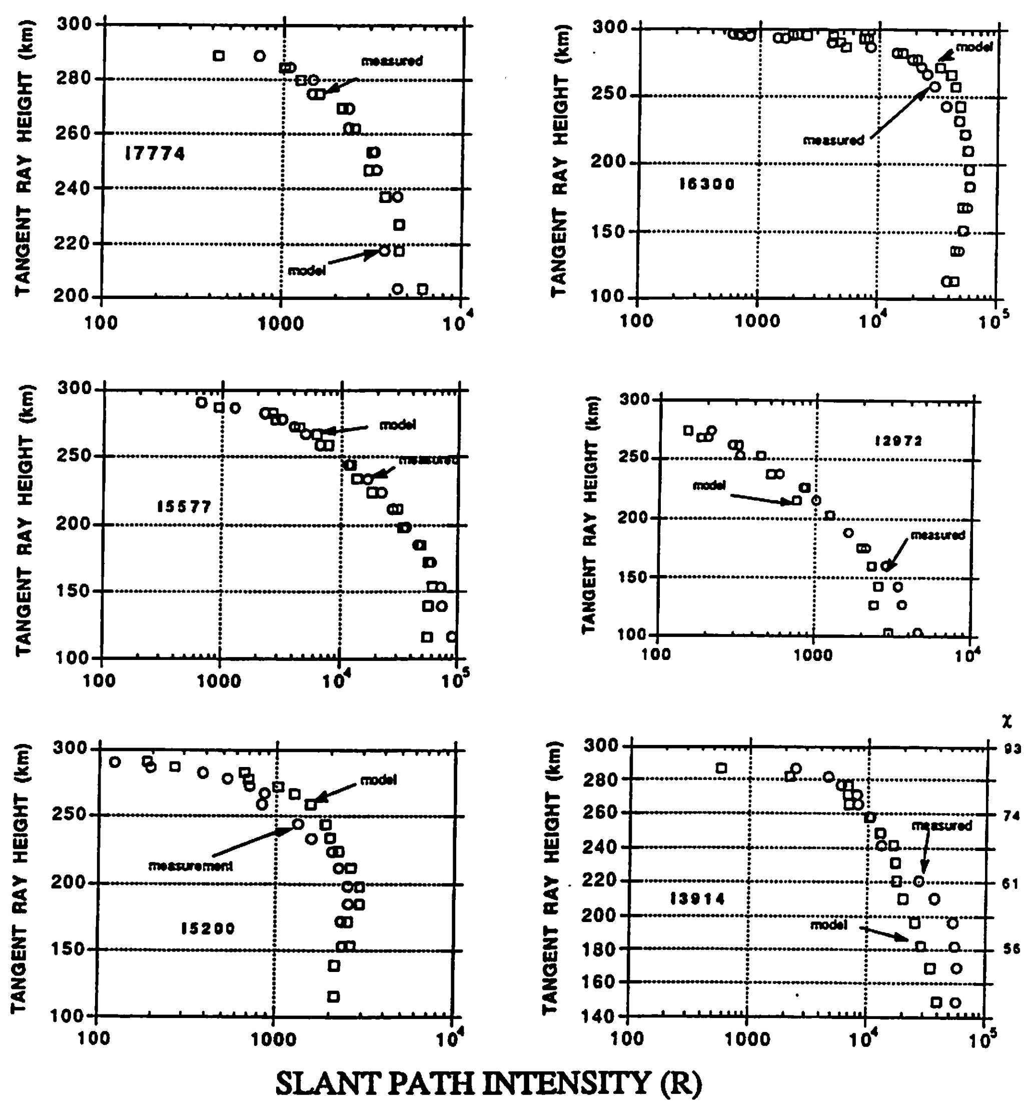


Fig. 3. Comparison of measured and modeled slant path intensity for: OI 7774 Å, OI 6300 Å, OI 5577 Å, OI 2972 Å, NI 5200 Å, and $N_2^+$ 1N 3914 Å. The variation of solar zenith angle is shown on the right-hand axis of the 3914 Å panel.

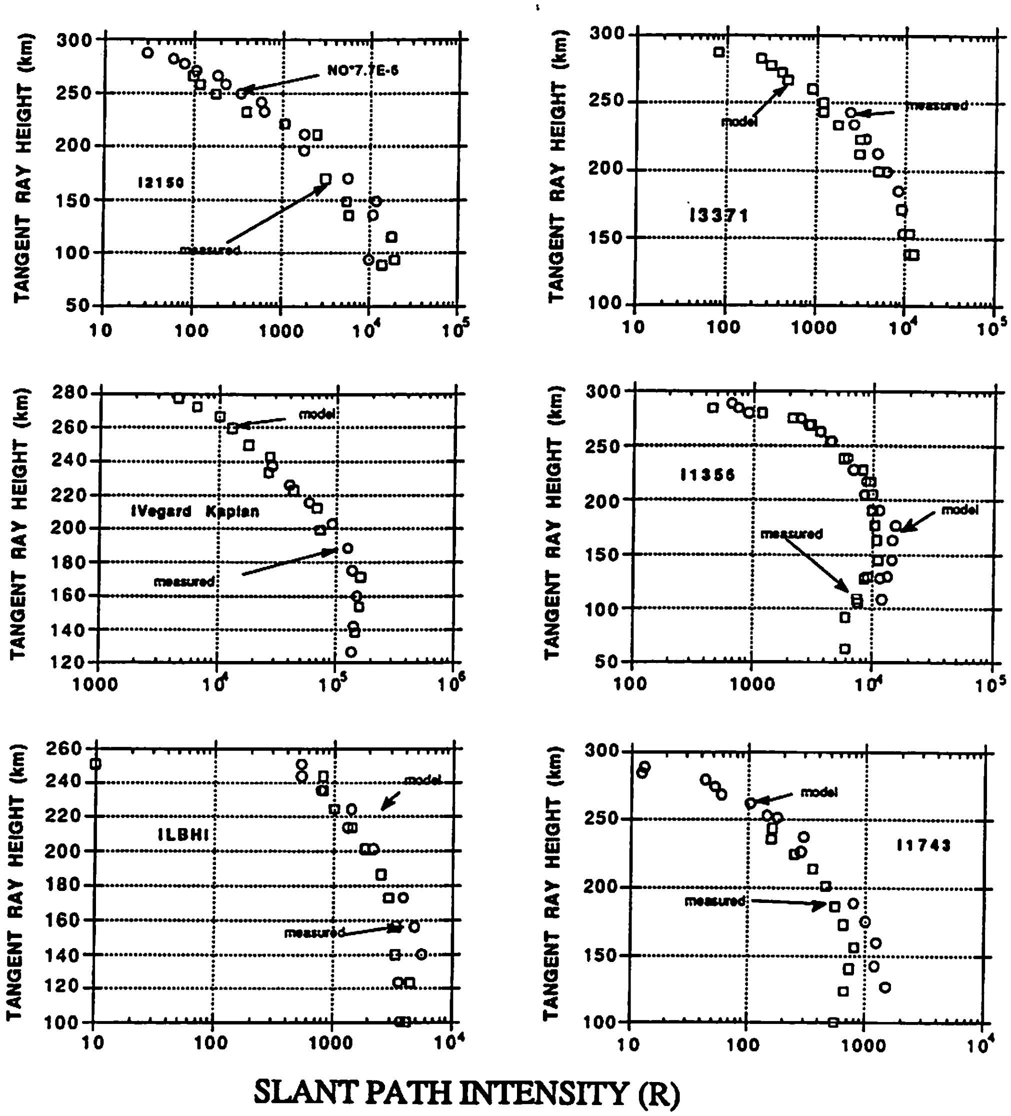


Fig. 4. Comparison of measured and modeled slant path intensity for: NO γ2150 Å, $N_2$ 2P 3371 Å, $N_2$ V-K (0-6, 0-7), OI 1356 Å, $N_2$ LBH 1670-1850 Å, NI 1743 Å.

emissions measured with an entirely different type of instrument almost 20 years later. This means that we are now in a good position to similarly establish the photochemistry of the lower thermosphere and mesosphere.

Acknowledgements. We thank the crew of the ATLAS-1 mission; Charles Bolden, Brian Duffy, and David Leestma, for their care in executing the maneuvers necessary to acquire these data; Kathy Sullivan, Michael Foale, Byron Lichtenberg, and Dirk Frimont for their assistance during the operations. This work was supported by contract NAS8-37106 to the University of Alabama in Huntsville.

References

Hedin, A. E., MSIS-86 thermospheric model, *J. Geophys. Res., 92*, 4649, 1987.

Torr, M. R., R. W. Basedow, and D. G. Torr, Imaging spectroscopy of the thermosphere from the space shuttle, *Appl. Optics, 21*, 4130, 1982.

Torr, M. R., R. W. Basedow, and J. Mount, An imaging spectrometric observatory for Spacelab, *Astrophys. Space Sci., 92*, 237, 1983.

Torr, M. R., D. G. Torr, P. G. Richards, and S. P. Young, Mid- and low-latitude model of thermospheric emissions, 1, $O^+(^2P)$ 7320 Å and $N_2(^2P)$ 3371 Å, *J. Geophys. Res., 95*, 21,147, 1990.

Torr, M. R., D. G. Torr, T. Chang, P. G. Richards, T. W. Baldridge, J. K. Owens, H. Dougani, C. Fellows, W. Swift, S. Yung, and J. Hladky, The first negative bands of $N_2^+$ in the dayglow from the ATLAS-1 shuttle mission, *Geophys. Res. Lett.*, this issue, 1993.

P. G. Richards and D. G. Torr, Center for Space Plasma and Aeronomic Research, University of Alabama in Huntsville, Huntsville, AL 35899.

M. R. Torr, Space Science Laboratory, NASA Marshall Space Flight Center, Huntsville, AL 35812.

(Received February 15, 1993;
accepted March 3, 1993)

# PHOTOCHEMICAL SYSTEMS

MAJOR SPECIES (O, $O_2$, $N_2$)

RESERVOIR MOLECULES (*eg*. $H_2O$, $H_2$)

METASTABLE NEUTRALS

PERMITTED EXCITED STATES

ODD HYDROGEN FAMILY

ODD OXYGEN FAMILY

ODD NITROGEN FAMILY

METALLIC NEUTRALS AND IONS

MAJOR AND MINOR IONIC SPECIES

METASTABLE IONS

CLUSTER IONS

TRACER SPECIES

## MESOSPHERE LOWER THERMOSPHERE PHOTOCHEMICAL SYSTEMS

| SYSTEM | MEMBERS | REGION | ROLE |
|---|---|---|---|
| MAJOR SPECIES | O, $O_2$, $N_2$ | MLTI | ENERGY ABSORBERS, REACTANTS<br>START OF PHOTOCHEMICAL CHAIN |
| METASTABLE NEUTRALS | $O(^1D)$, $O(^1S)$, $N(^2D)$, $N(^2P)$ | MLT | ENERGY STORAGE/TRANSFER |
| | $N(^2P)$, $N_2^*(V)$, $O_2^*(V)$, $N(^2A)$ | | KINETICS MODERATORS |
| | $O_2$(A, A' ,C1 , a, b), $OH^*$ | | RADIATORS/HEAT LOSS |
| | $CO_2$(VIB) | | OBSERVABLES |
| EXCITED STATES | O, $O_2$, $N_2$, N, OH, NO | | RADIATORS/HEAT LOSS |
| | | | METASTABLE SOURCES |
| ODD OXYGEN (Ox) | O | M | SINGLE SOURCE OF $O_3$ |
| | | | KEY REACTANT |
| | | | RADIATOR/HEAT SINK |
| | | | CHEMICAL HEAT SOURCE |
| | $O_3$ | M, STRAT | UV ENERGY ABSORBER, RADIATOR, REACTANT |
| | | | CLIMATOLOGY CONTROL |
| | | | D REGION ION CHEMISTRY |
| ODD HYDROGEN | H, OH, $HO_2$, (HOx) | M | CATALYTIC Ox DESTRUCTION |
| | | | CHEMICAL HEAT SOURCES |
| HOx RESERVOIRS | $H_2O$, $H_2$ | | HOx PHOTOCHEMICAL SOURCES |
| ODD NITROGEN | N, $N(^2D)$, $N(^4S)$, NO, $NO_2$ | LT | HEAT SOURCES AND TRANSFER, REACTANTS |
| | $N(^2D)$ | LT | OBSERVABLE FOR $NO^+$ |
| | NO | LT | SOURCE OF $NO^+$ |
| | | MLT | RADIATOR/HEAT SINK |
| | | MLT | SOURCE OF STRAT NO |
| | | STRAT | $O_3$ CATALYTIC DESTRUCTION |
| METALLIC NEUTRALS | Na, Ca, K, Fe | M | OBSERVABLES/TRACERS |
| MAJOR IONS | $O^+$, $O_2^+$, $NO^+$, $N_2^+$ | MLTI | REACTANTS/HEAT SOURCES |
| MINOR IONS | $N^+$ | LT | MINOR REACTANT |
| METASTABLE IONS | $O^+(^2D)$ | LT | CHEMICAL ENERGY TRANSFER |
| | $O^+(^2P)$ | T | LT COMPOSITION MONITOR |
| METALLIC IONS | $Ca^+$, $Mg^+$, $Fe^+$ | MLTI | DYNAMICS TRACERS |

# THE HYDROGEN-OXYGEN SYSTEM

**Odd Oxygen Photochemistry (Chapman, 1930)**

**Hydrogen-Oxygen (Bates and Nicolet, 1950)**

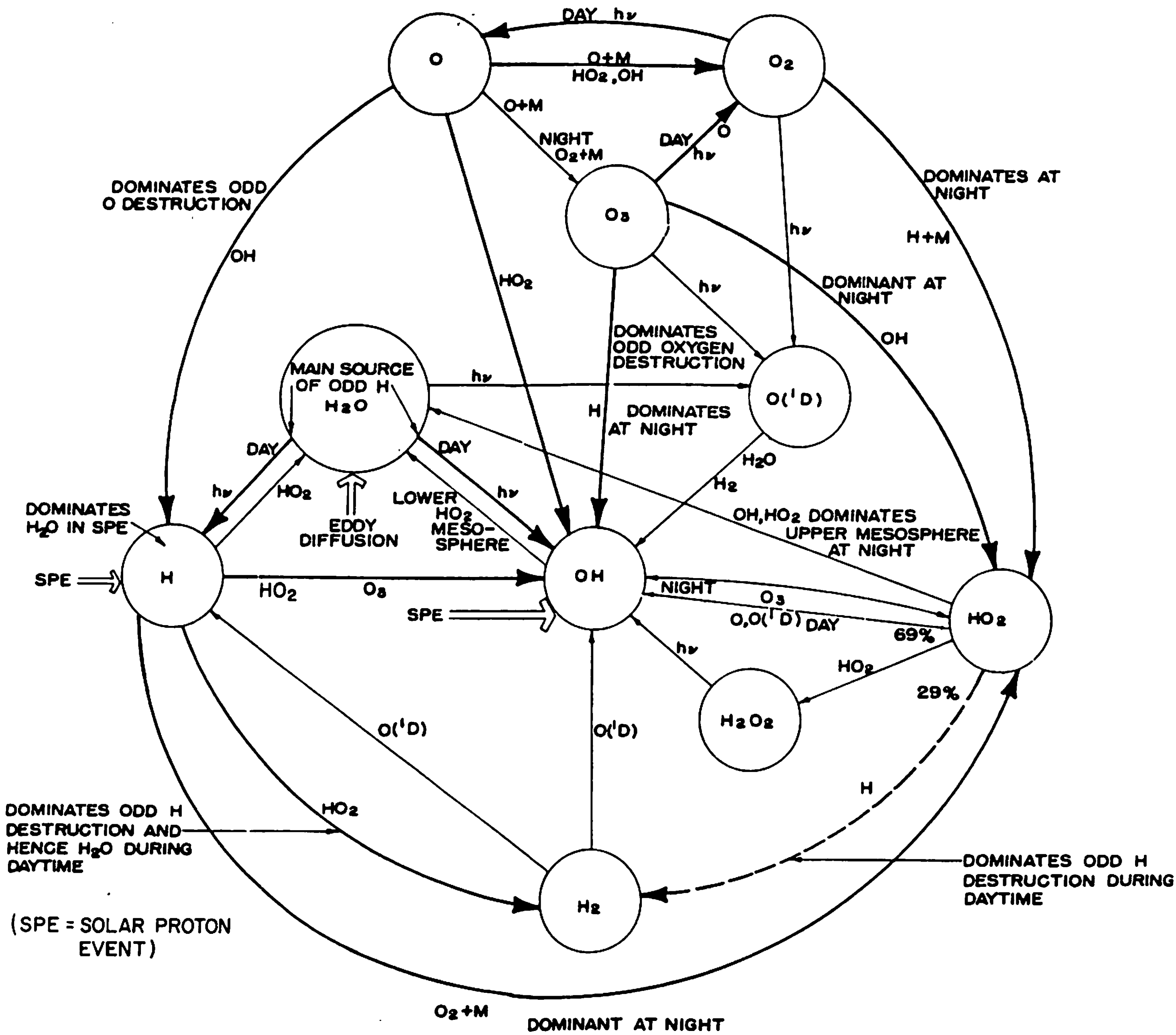


MESOSPHERIC OXYGEN-HYDROGEN CHEMISTRY

# ROLE OF KEY OXYGEN-HYDROGEN CONSTITUENTS IN THE MLTI

| ID | KEY PROCESSES | REGION | KEY ROLES |
|---|---|---|---|
| O | $O + h\nu$ | LTI | Ion Chemistry; Photoionization $\rightarrow O^+(^4S, ^2D, ^2P)$ |
| | $O + N_2^+$ | LTI | Ion Atom interchange Conversion of $N_2^+$ to $NO^+$ |
| | $O + e \rightarrow O^* + e$ | LTI | Source of Excited Metastable $O(^1D)$, $O(^1S)$ and Permitted States |
| | $O^* \rightarrow O + h\nu$ | LT | Radiative Sink |
| | $O + X^* \rightarrow X + O$ | LTI | Quenches $N_2(A)$, $O(^1D, ^1S)$, $N(^2D, ^2P)$, $O^+(^2D, ^2P)$, $N_2^*$, $O_2^*$ |
| | | | LT Heat Source |
| | $O + O + M \rightarrow O_2$ | MLT | Heat Reservoir; Source of $O_2(C^1, A, A') \rightarrow$ Precursors to Several emissions |
| | $O + O_2^* \rightarrow O_2'$ | MLT | Quenches $O_2(A, A', C^1, a, b)$ |
| | $O + O_2 + M \rightarrow O_3$ | MLT | Only Source of Ozone $\rightarrow$ Primary Mesospheric Heat Source |
| | $O + O_3 \rightarrow O_2 + O_2$ | MLT | Destruction of Ox |
| | $O + OH \rightarrow H + O_2$ | MLT | Step in Catalytic Destruction of Ozone and Ox Loss Cycle |
| | | | MLT Heat Source |
| | $O + M \rightarrow O^* + M$ | MLTI | Fine Structure Excitation |
| | $O^* \rightarrow O$ (63 μm) | MLTI | Fine Structure Cooling |
| | $O + CO_2^* \rightarrow CO_2 + O$ | MLT | Energy Transfer to $CO_2 \rightarrow$ Radiative Loss |
| $O_3$ | $O_3 + h\nu \rightarrow O(^1D) + O_2(^1\Delta)$ | M | Absorption of UV Energy; Mesospheric Heat Source + Excitation |
| | | | Radiative Loss $\rightarrow$ Heat Sink and Observable Emissions |
| | | | UV Absorption $\rightarrow$ Observable Signature for O3 Measurement |
| $H_2O$ | $H_2O + h\nu \rightarrow OH + O$ | MLT | Source of Mesospheric HOx; Drives Hydrogen-Oxygen Chemistry |
| | $H_2O + O(^1D) \rightarrow$ | MLT | Minor Source of Mesospheric OH |
| | $H_2O + O_2^+ + e \rightarrow$ | MLT | $O_2 + H + OH$; Storm Time Enhancement of HOx Through Ion Clusters |
| H | $H + O_3 \rightarrow OH^* + O_2$ | MLT | First Step in Catalytic Destruction of O3; Heat Source |
| | | | Source of Meinel Bands $\rightarrow$ O3 Destruction Rate or H Density |
| | $H + HO_2 \rightarrow H_2O + O$ | M | HOx Destruction |
| | $H + O_2 + M \rightarrow HO_2$ | M | HOx Partitioning |
| OH | $OH + O \rightarrow H + O_2$ | MLT | 2nd Step in Catalytic Destruction of O3; Heat Source ***** |
| | | | OH Moderates the NO and Cl Anthropogenic Cycles in the Strat. |
| | $OH + OH \rightarrow H_2O + O$ | M | HOx Destruction |
| | $OH + HO_2 \rightarrow H_2O + O_2$ | M | HOx Destruction |

MLT MEASUREMENTS OF H, OH, O AND $H_2O$ ARE SPARSE.

## CATALYTIC DESTRUCTION OF ODD OXYGEN BY ODD-HYDROGEN

$$O_3 + H \rightarrow OH + O_2$$
$$OH + O \rightarrow H + O_2$$
$$\overline{O + O_3 \rightarrow 2O_2}$$

$$HO_2 + O \rightarrow OH + O_2$$
$$OH + O \rightarrow H + O_2$$
$$H + O_2 + M \rightarrow HO_2 + M$$
$$\overline{O + O \rightarrow O_2}$$

## PRODUCTION AND DESTRUCTION OF ODD-HYDROGEN RADICALS

$$H_2O + h\nu \xrightarrow{J_5} H + OH$$

$$H_2O + O(^1D) \xrightarrow{k_8} OH + OH^*_{(\nu \geq 2)}$$

$$HO + HO_2 \xrightarrow{k_{9a}} H_2O + O_2$$

$$OH + OH \xrightarrow{k_{9b}} H_2O + O$$

$$H + HO_2 \xrightarrow{k_{10}} H_2O + O$$

$$H + HO_2 \xrightarrow{k_{11}} H_2 + O_2$$

# WATER VAPOR

The upward transport of $H_2O$ is balanced by photochemical conversion to H and $H_2$ via

$$H_2O + h\nu \longrightarrow H + OH$$

$$OH + O \longrightarrow H + O_2$$

$$H_2O + O \longrightarrow 2H + O_2$$

$$H_2O + h\nu \longrightarrow H + OH$$

$$O + OH \longrightarrow H + O_2$$

$$H + O_2 + M \longrightarrow HO_2 + M$$

$$H + HO_2 \longrightarrow H_2 + O_2$$

$$H_2O + O \longrightarrow H_2 + O_2$$

In the paper "The Vertical Distribution of Ozone in the Mesosphere and Lower Thermosphere" by M. Allen, J. I. Lunine, and Y. L. Yung (*Journal of Geophysical Research*, *89*(D3), 4841–4872, 1984) the shading in Figures 11 and 12 was not reproduced. Both figures are reproduced in better detail below. See the original article for captions.

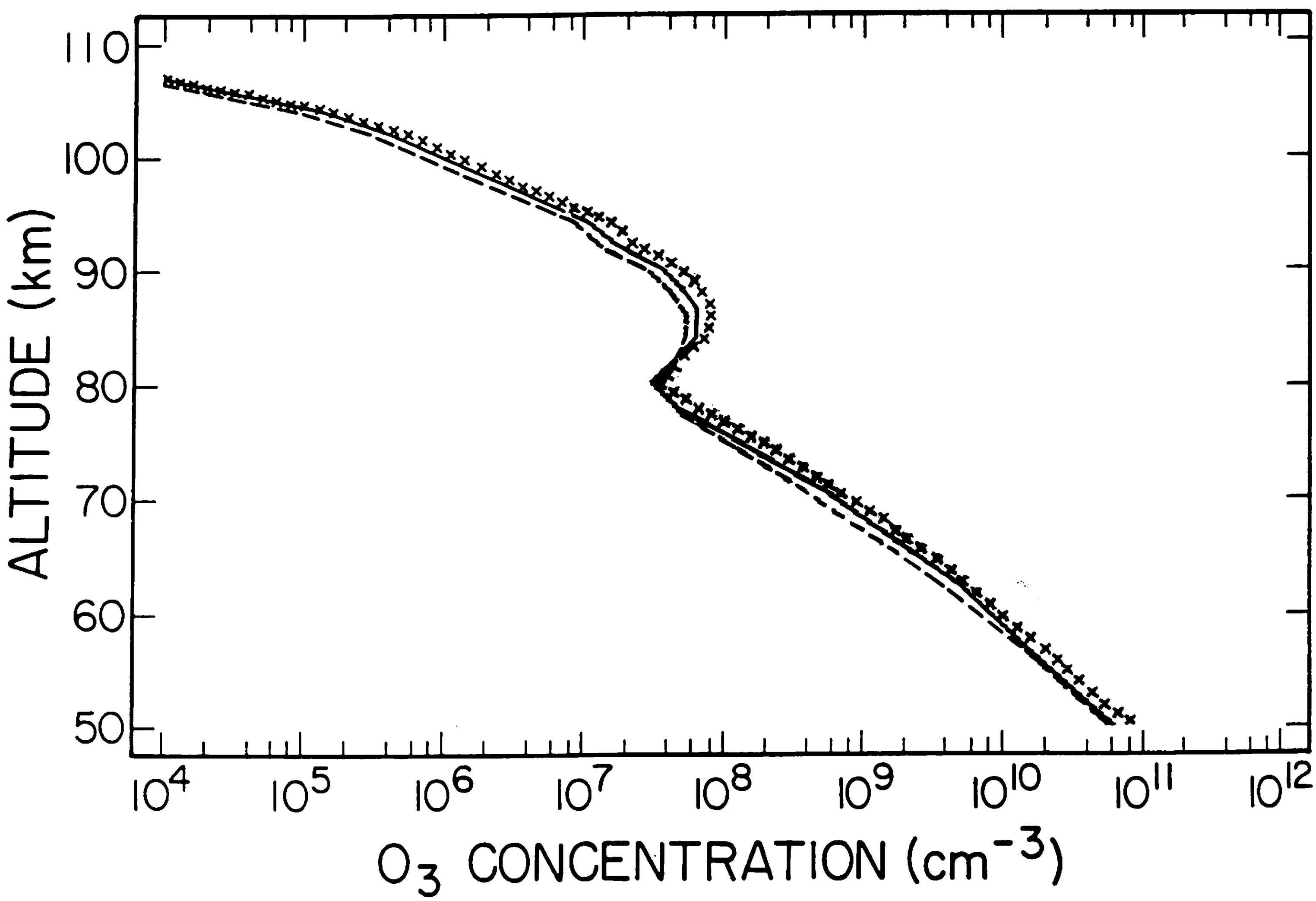

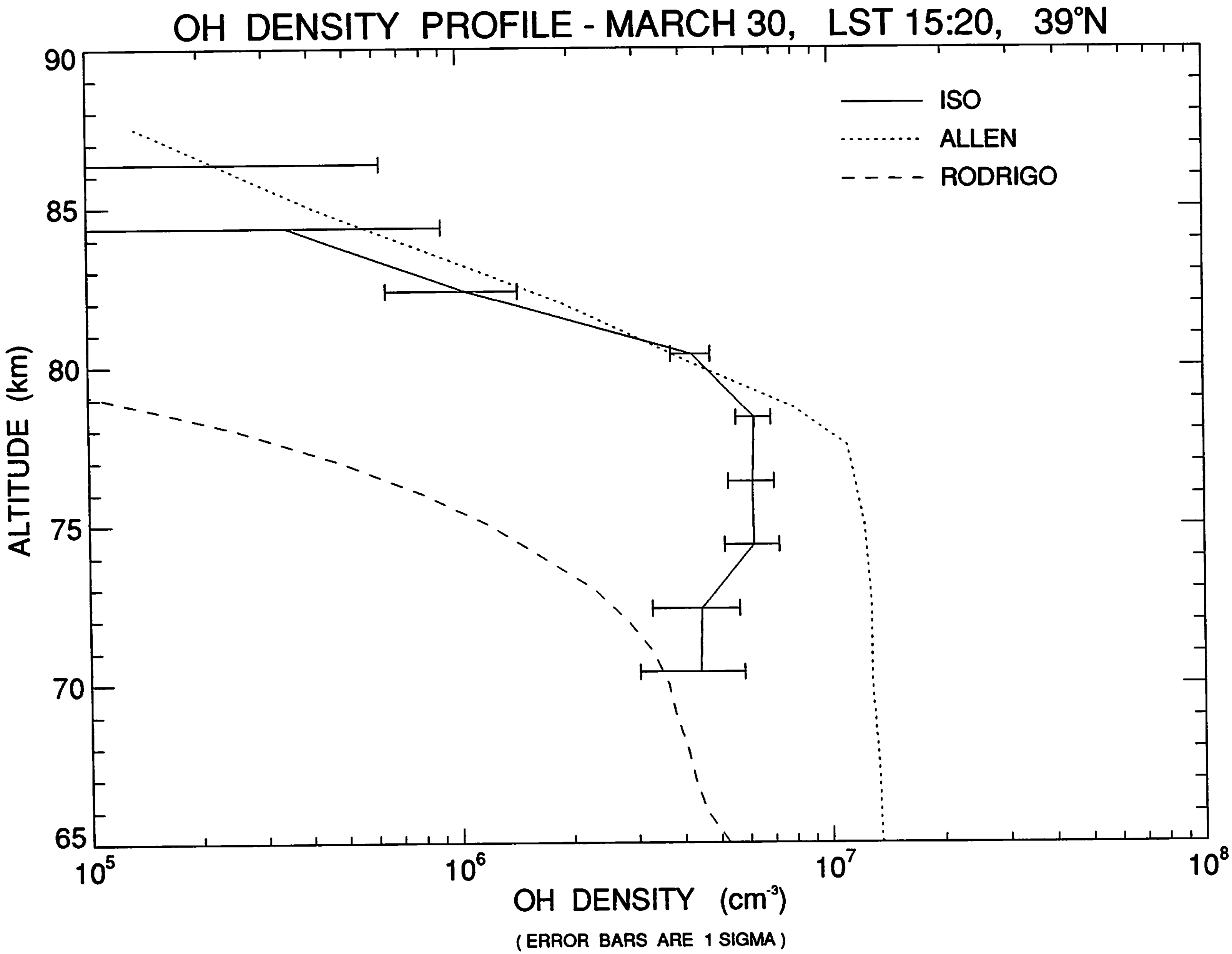
OH DENSITY PROFILE - MARCH 30, LST 15:20, 39°N
ISO
ALLEN
RODRIGO
ALTITUDE (km)
90
85
80
75
70
65
10^5
10^6
10^7
10^8
OH DENSITY (cm^-3)
( ERROR BARS ARE 1 SIGMA )

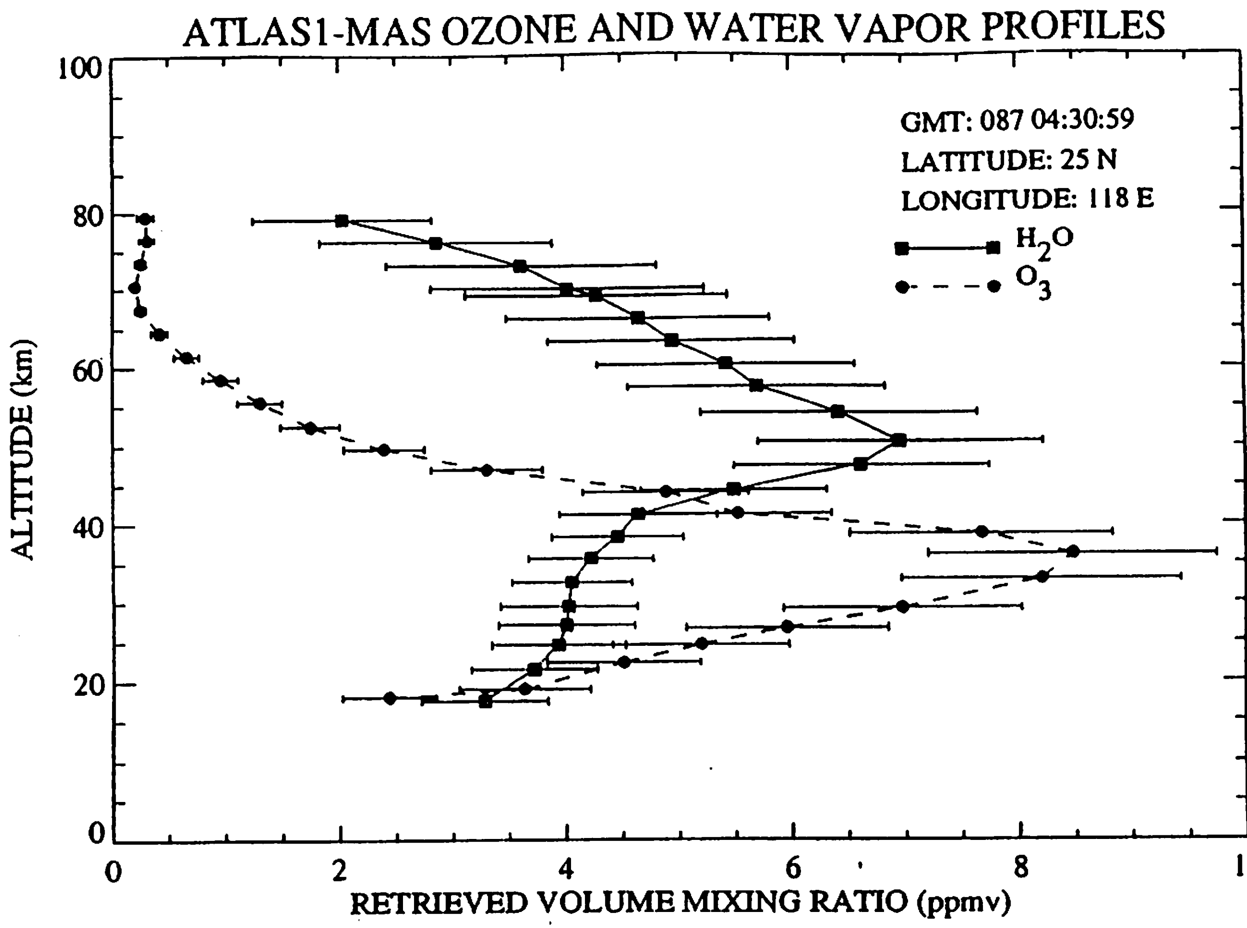
ATLAS1-MAS OZONE AND WATER VAPOR PROFILES
GMT: 087 04:30:59
LATITUDE: 25 N
LONGITUDE: 118 E
$H_2O$
$O_3$
ALTITUDE (km)
RETRIEVED VOLUME MIXING RATIO (ppmv)
0
20
40
60
80
100
0
2
4
6
8
10

Figure 5

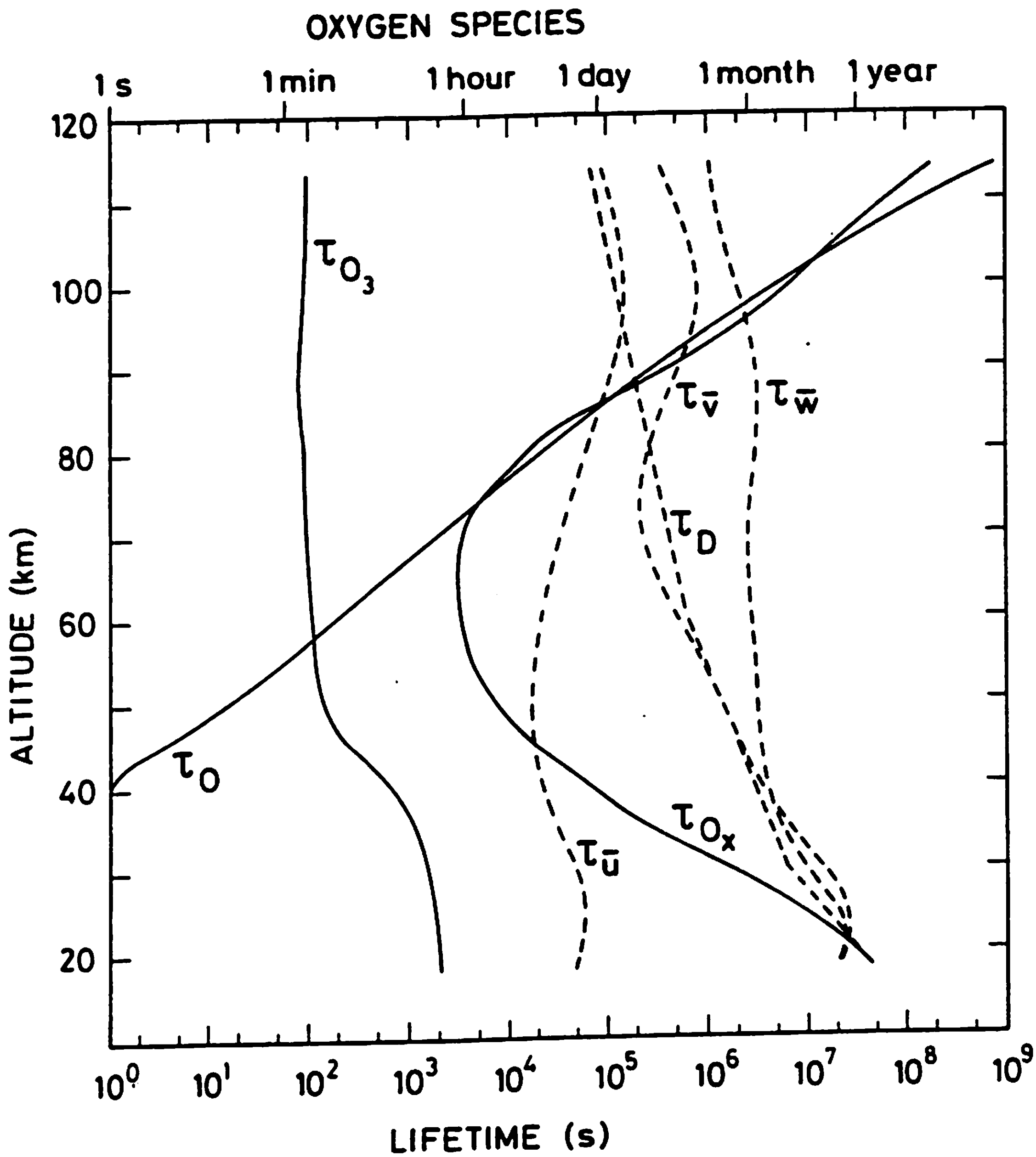


Photochemical lifetimes of $O_x$, $O_3$, and O, and characteristic transport lifetimes.

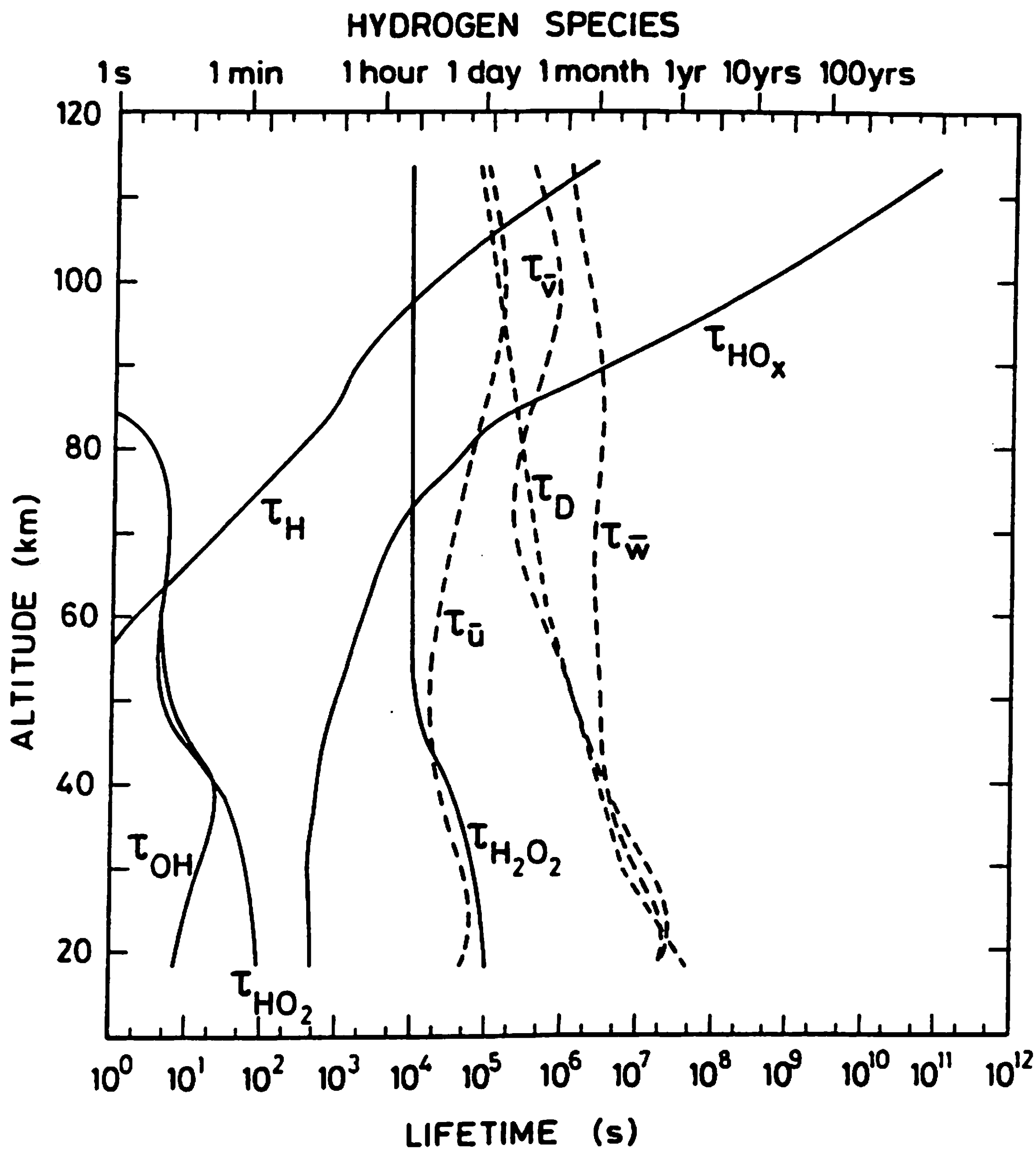


Photochemical lifetimes of $HO_x$, H, OH, $HO_2$, and $H_2O_2$, and the time constants for transport.

Neutral atmospheric composition (60–220 km)

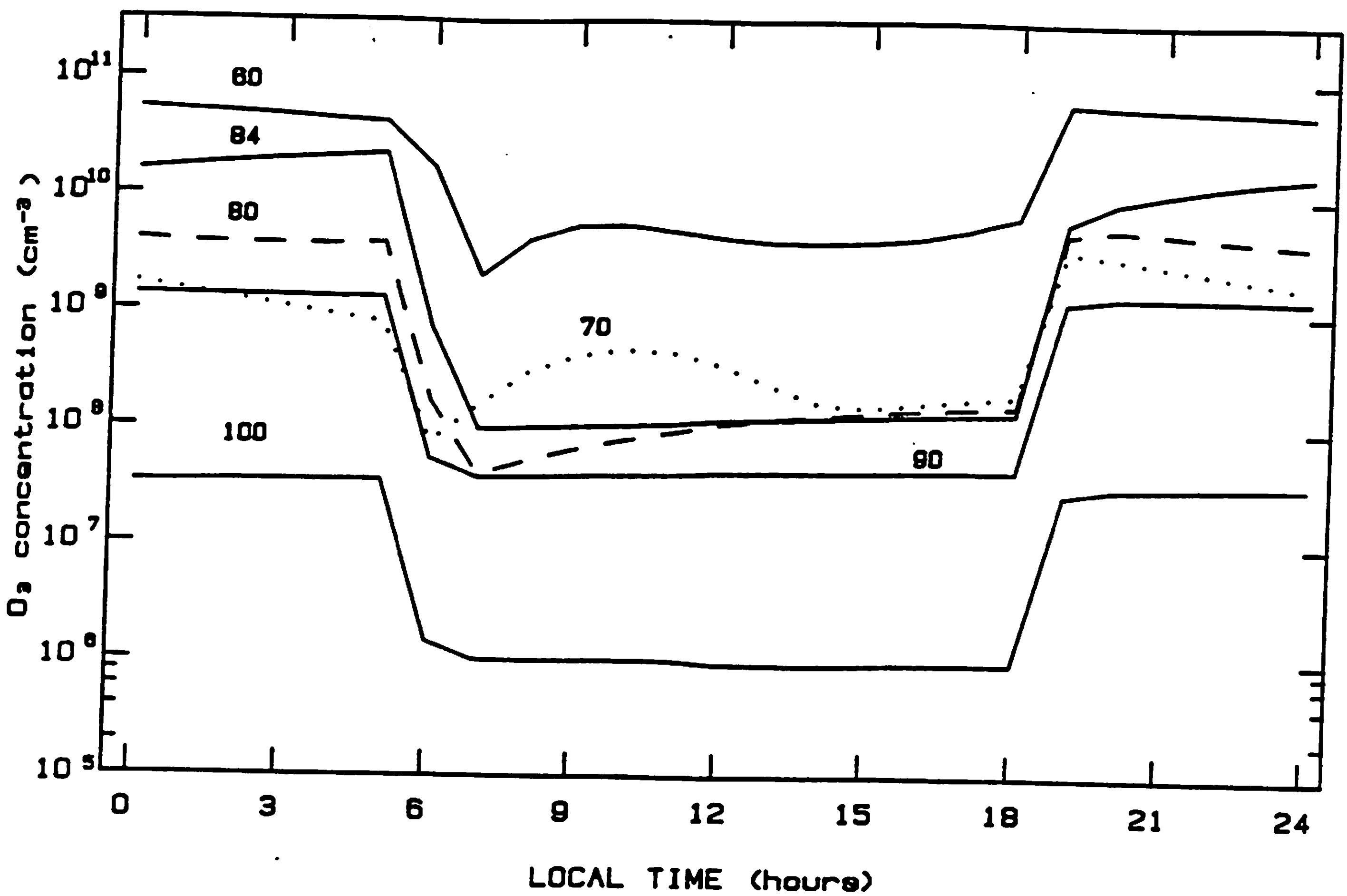


FIG. 13. DIURNAL VARIATION OF OZONE AT SELECTED ALTITUDES.

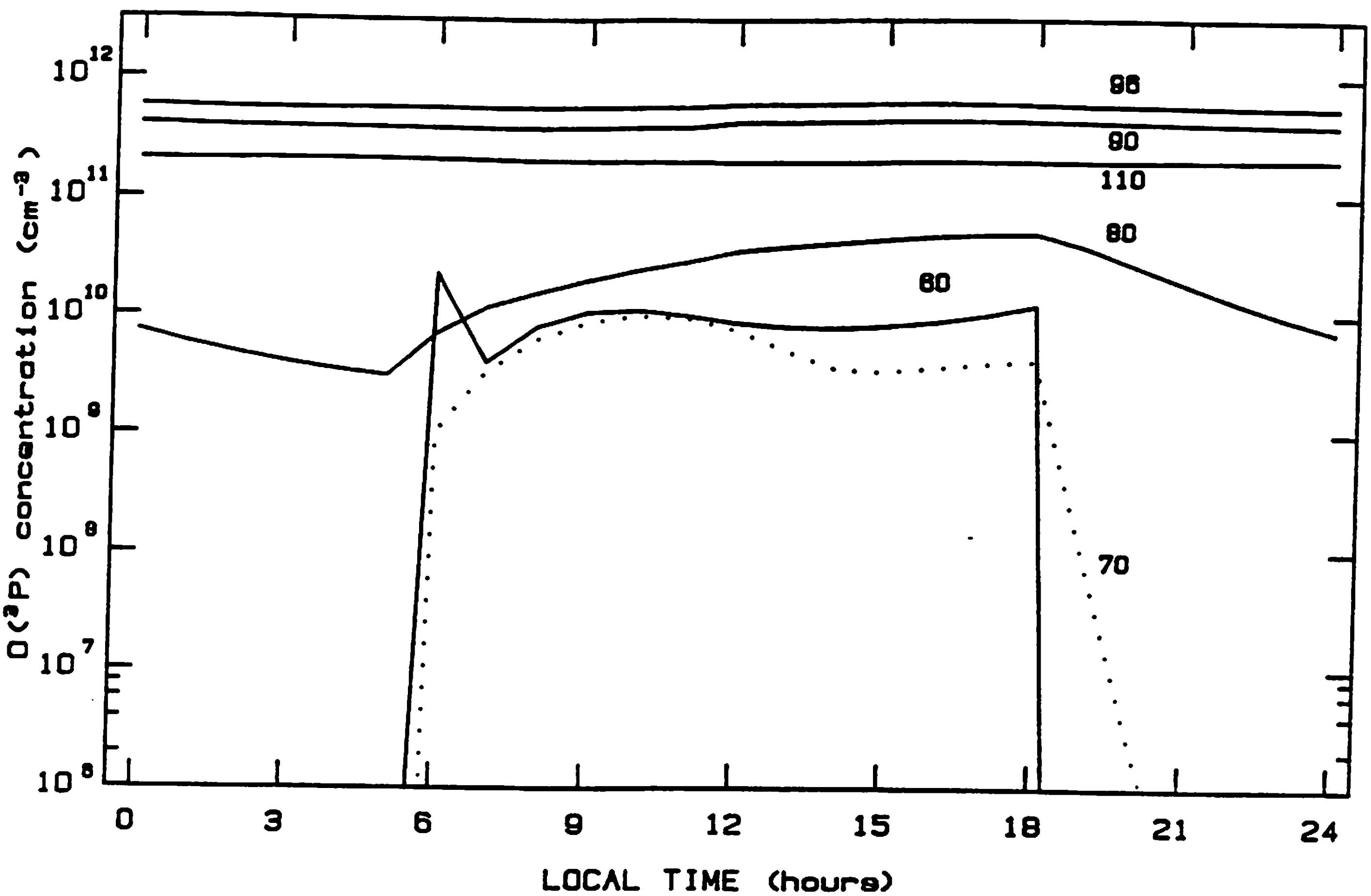


FIG. 11. DIURNAL VARIATION OF O($^3$P) AT SELECTED ALTITUDES.

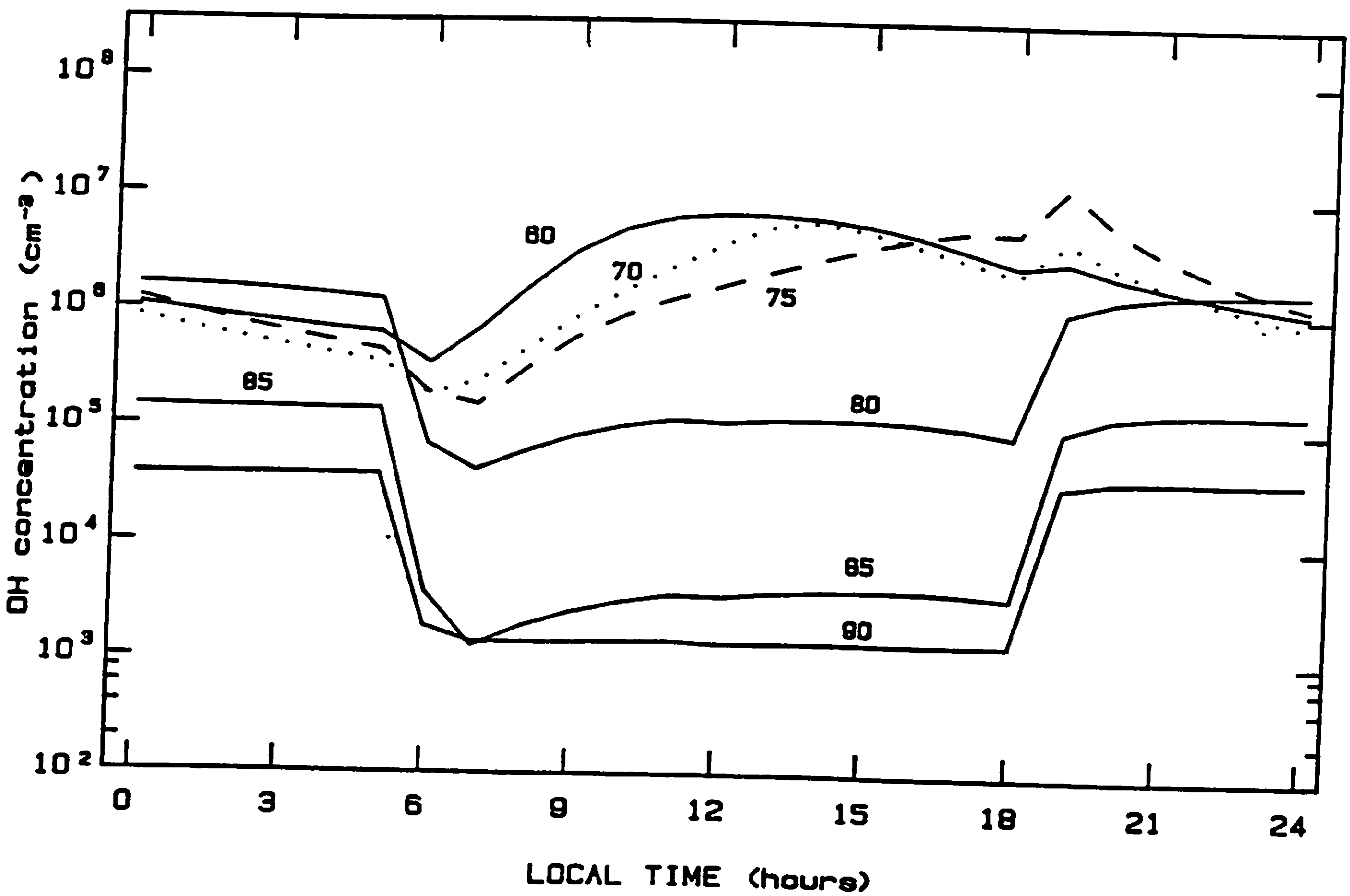


FIG. 15. DIURNAL VARIATION OF HYDROXYL MOLECULE AT SELECTED ALTITUDES.

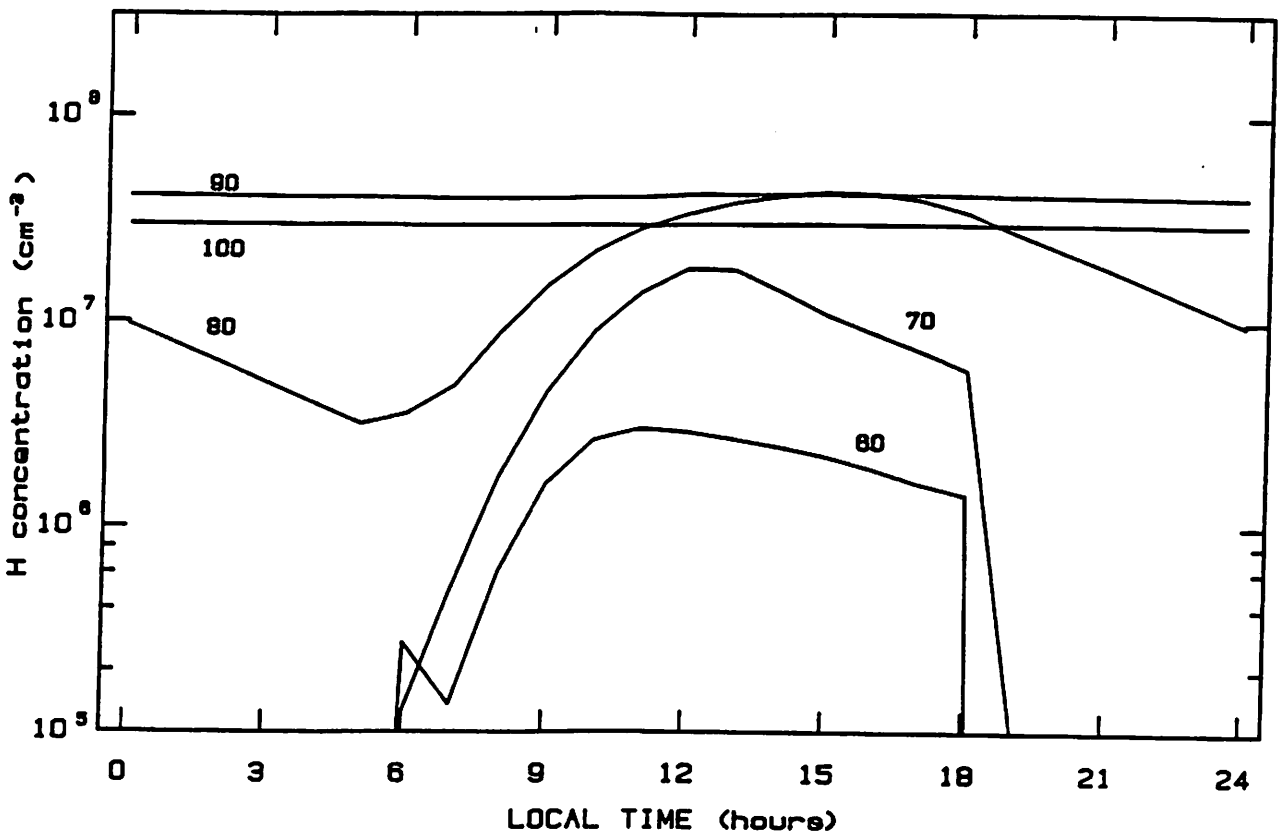


FIG. 17. DIURNAL VARIATION OF ATOMIC HYDROGEN AT SELECTED ALTITUDES.

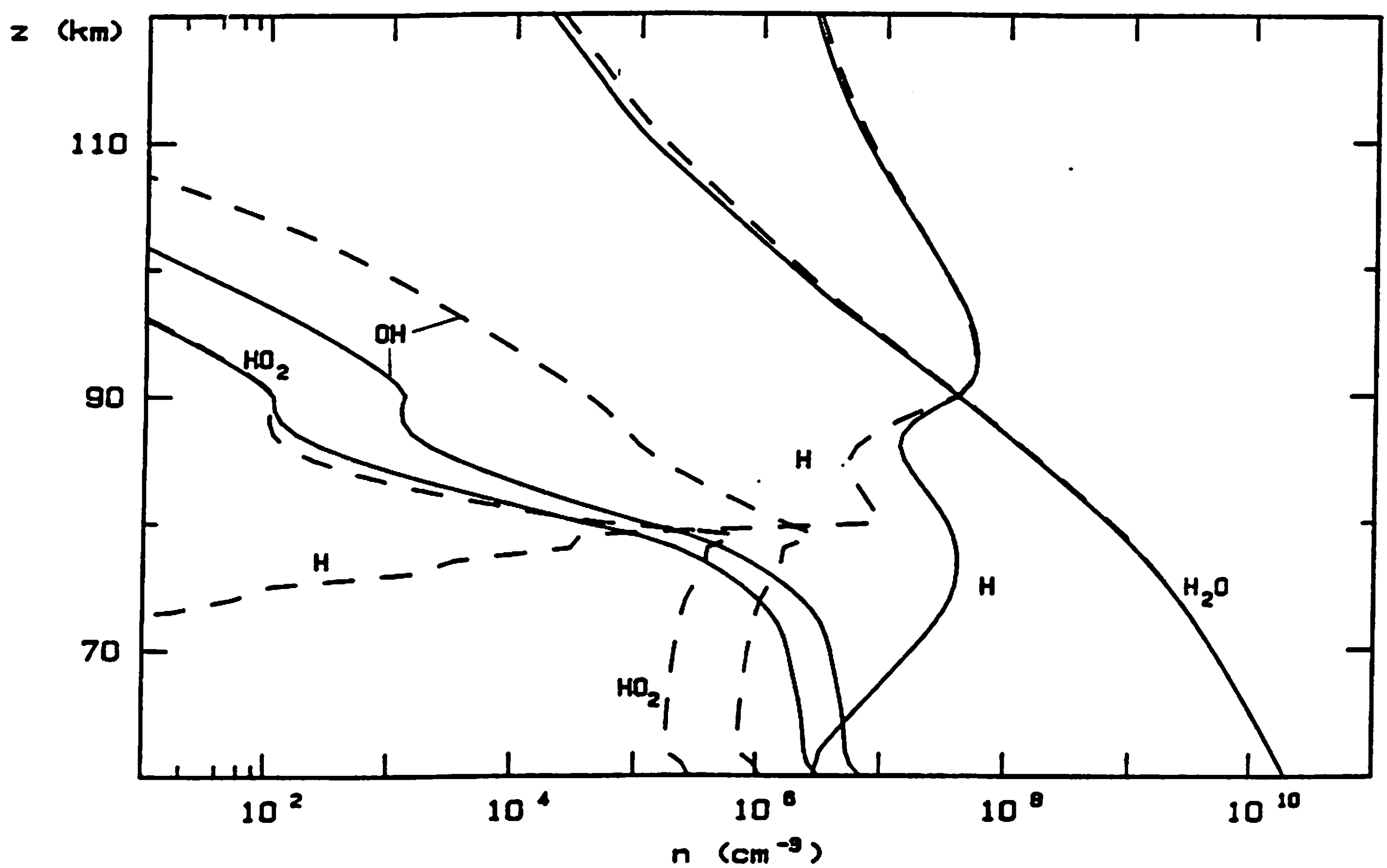


FIG. 14. H-COMPOUNDS CONCENTRATION PROFILES.
Solid lines, noon. Dashed lines, midnight.

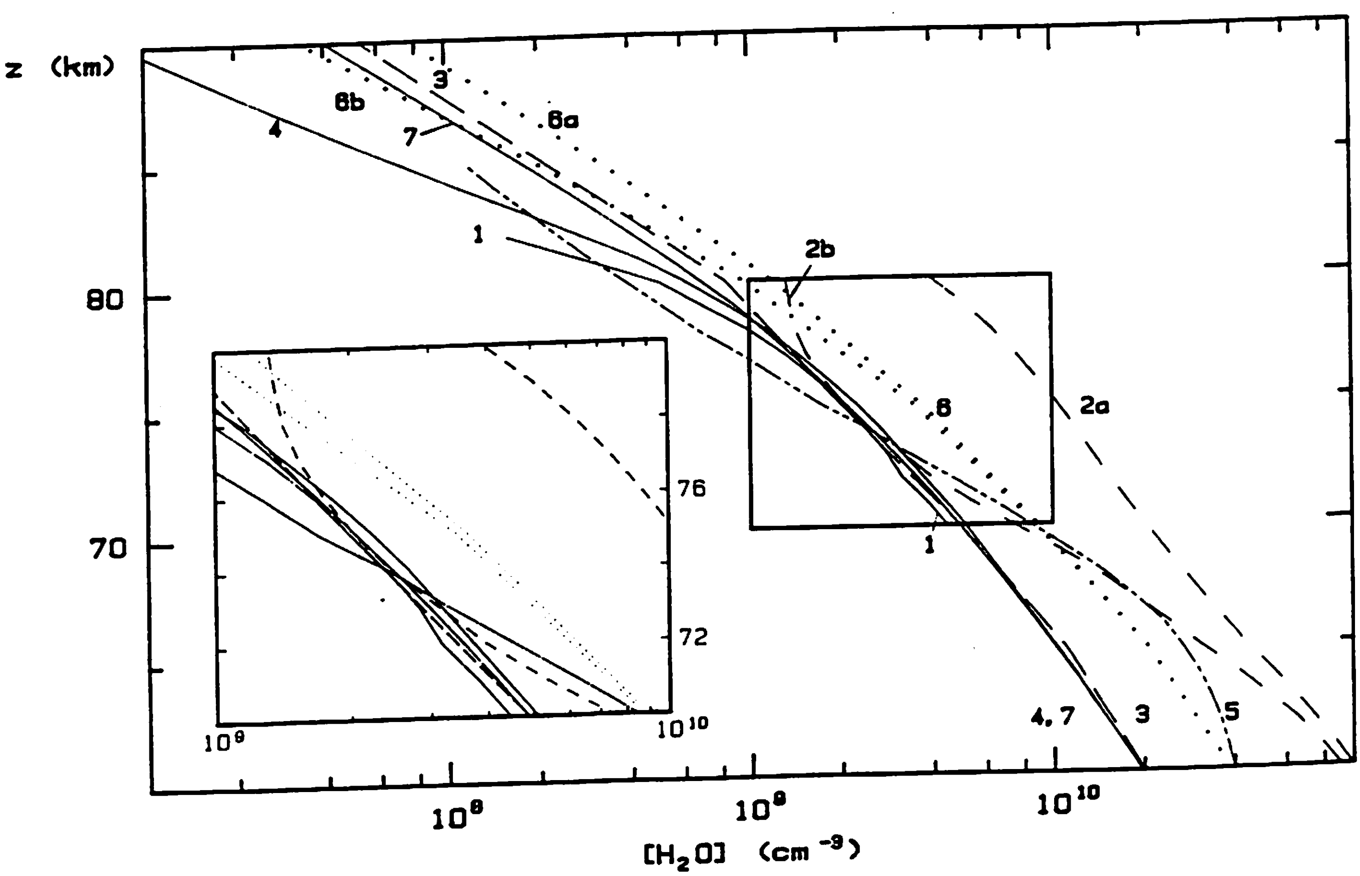


FIG. 18. DIFFERENT WATER VAPOR CONCENTRATION PROFILES.

Curve 1: Swider and Narcisi (1975). Curves 2a and b: Radford *et al.* (1977). Curve 3: Keneshea *et al.* (1979). Curve 4: Battaner and Rodrigo (1981). Curve 5: Gibbins *et al.* (1982). Curves 6a and b: Solomon *et al.* (1982). Curve 7: This model.

# MESOSPHERIC METASTABLE $O_2$ PHOTOCHEMISTRY

METASTABLE $O_2$ NIGHTTIME CHEMISTRY

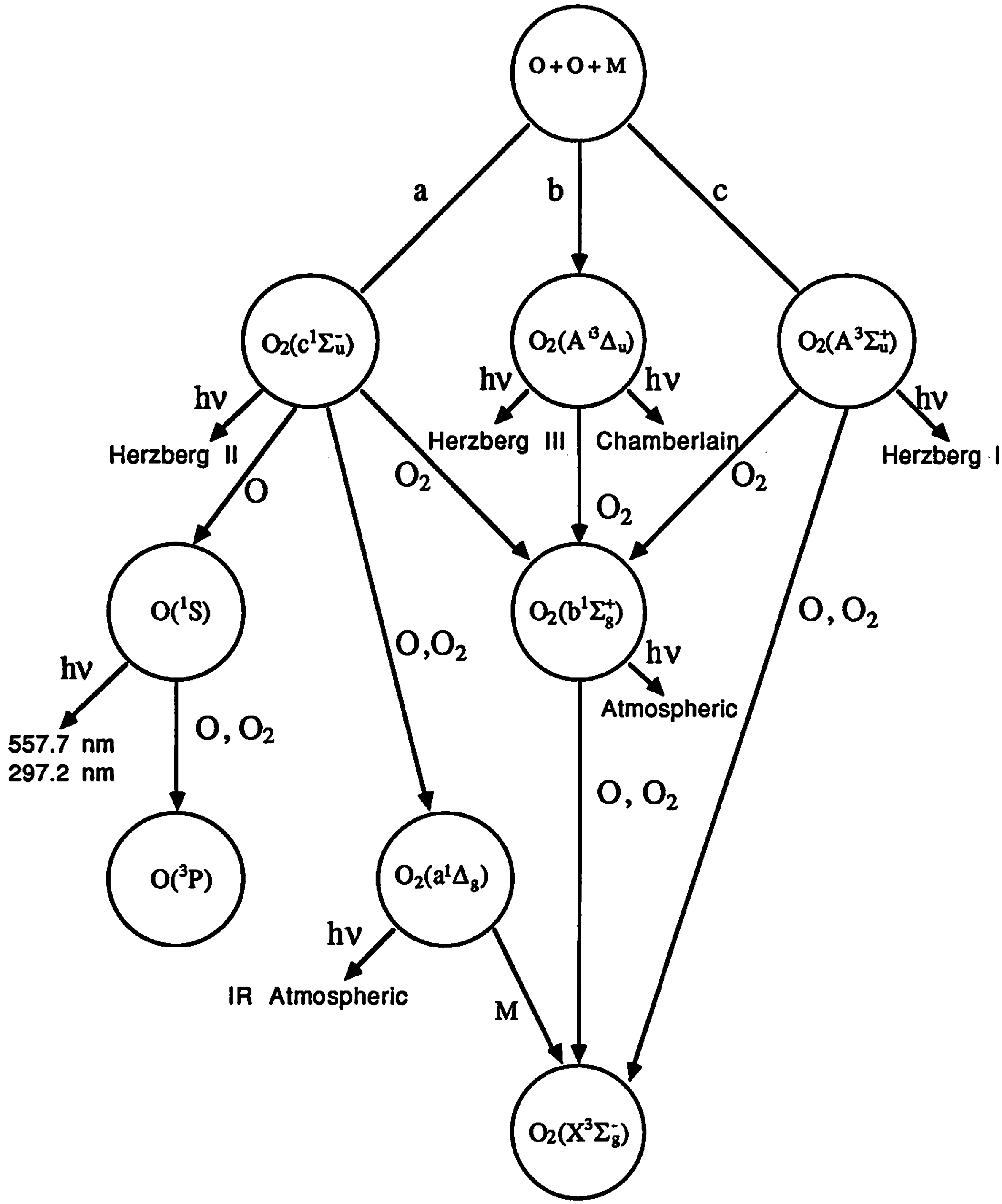

# EXCITATION MECHANISMS

**EXTENSIVELY STUDIED:**

BATES, 1964; LLEWELLYN *ET AL.*, 1979; THOMAS *ET AL.*, 1979; THOMAS, 1981, MURTAGH *ET AL.*, 1986a, b; KRASNOPOLSKY, 1986; BATES, 1988a, b, 1992.

RECENT MEASUREMENTS SUPPORT THE DIRECT EXCITATION THROUGH THREE-BODY O RECOMBINATION.

THOMAS, 1981; *ET AL.*, 1986a (ETON CAMPAIGN); SISKIND AND SHARP, 1991.

**MODEL RESULTS:**

PRODUCTION EFFICIENCY (ε) AND QUENCHING RATES (K)

⟶ ABSOLUTE INTENSITIES
LOW ε AND K ⟶ LOWER PEAK EMISSION HEIGHTS

GROUNDBASED AND ROCKETBORNE AIRGLOW MEASUREMENTS ⟶ LAB QUENCHING RATES ARE LOW

CONFIRMED BY RECENT SRI RESULTS FOR $O_2$(A)
V' = 7, 8, 9 FOR $O_2$ AND $N_2$ ⟶ HIGH RATES.

# PHOTOMETRIC ROCKET RESULTS

HEIGHT PROFILES

SUGGEST ALTITUDE INVARIANT VIBRATIONAL DISTRIBUTION (MEASUREMENTS FROM HIGH AND LOW VIBRATIONAL LEVELS)

DOUBLE PEAKED VIBRATIONAL DISTRIBUTION

CURRENT MODELS (BASED ON DEGEN, 1972)

3-BODY RECOMBINATION POPULATES $V' \geq 10$ FOLLOWED BY SINGLE QUANTA COLLISIONAL DEACTIVATION.

ALTITUDE INVARIANCE IN THE POPULATION DISTRIBUTION REQUIRES THE CASCADE AND ELECTRONIC QUENCHING SPECIES TO BE THE SAME

QUENCHING RATES >> RADIATIVE DECAY

$\Rightarrow$ HIGH $O_2$ QUENCHING RATES AND HIGH YIELDS

IF O QUENCHES ELECTRONIC STATES, IT MUST ALSO CAUSE SINGLE QUANTA VIBRATIONAL QUENCHING

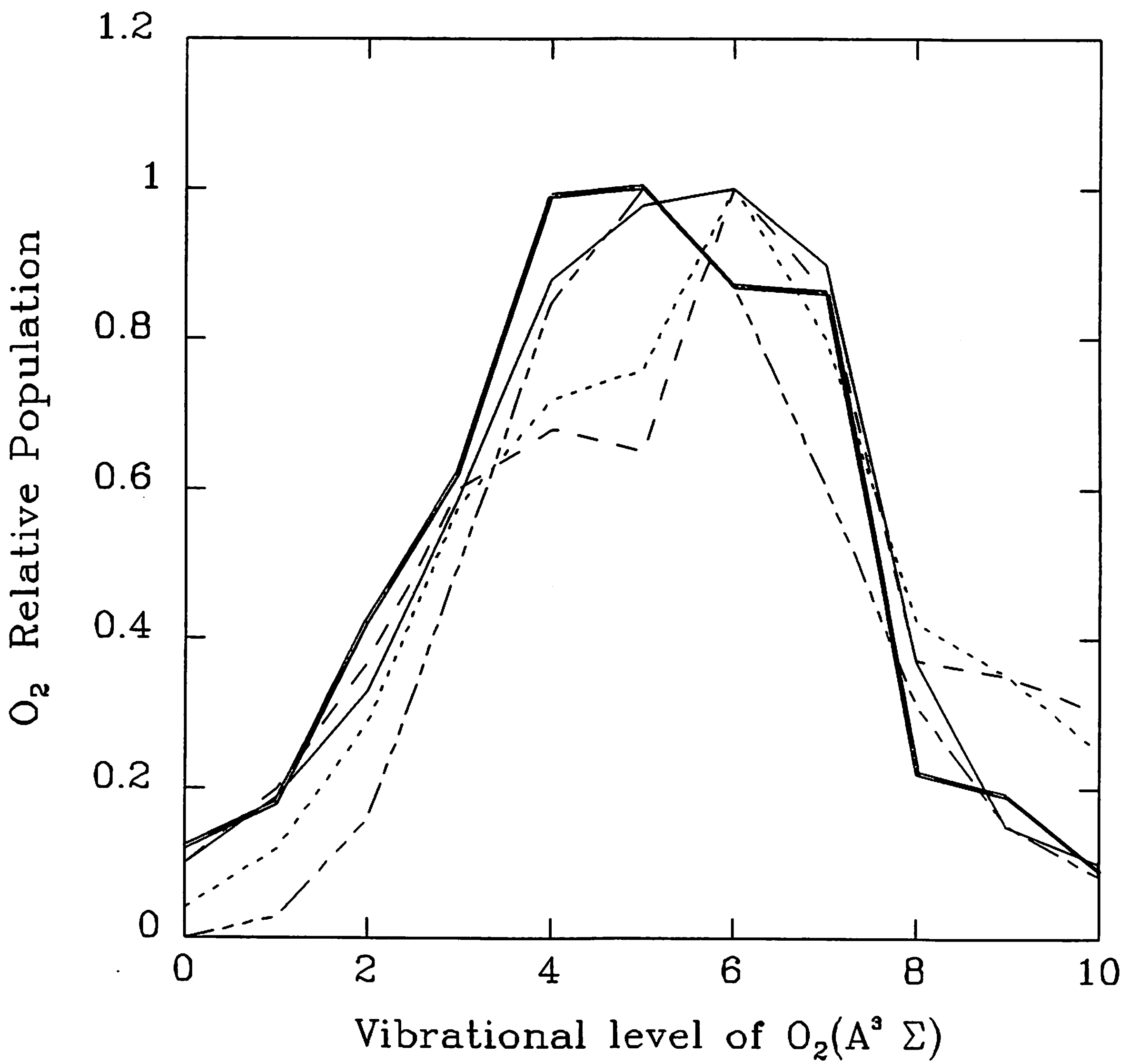


Vibrational populations. Thick solid curve: ISO distribution; Long dashed lines: Stegman and Murtagh [1991]; Thin solid line: Slanger and Heustis [1981]; Long dash, three short dashes: Lopez-Gonzales *et al.* [1992]: Model with electronic deactivation vibration independent rate coefficients; Dotted Line: Lopez-Gonzales *et al.* [1992]: Model with electronic deactivation vibration dependent.

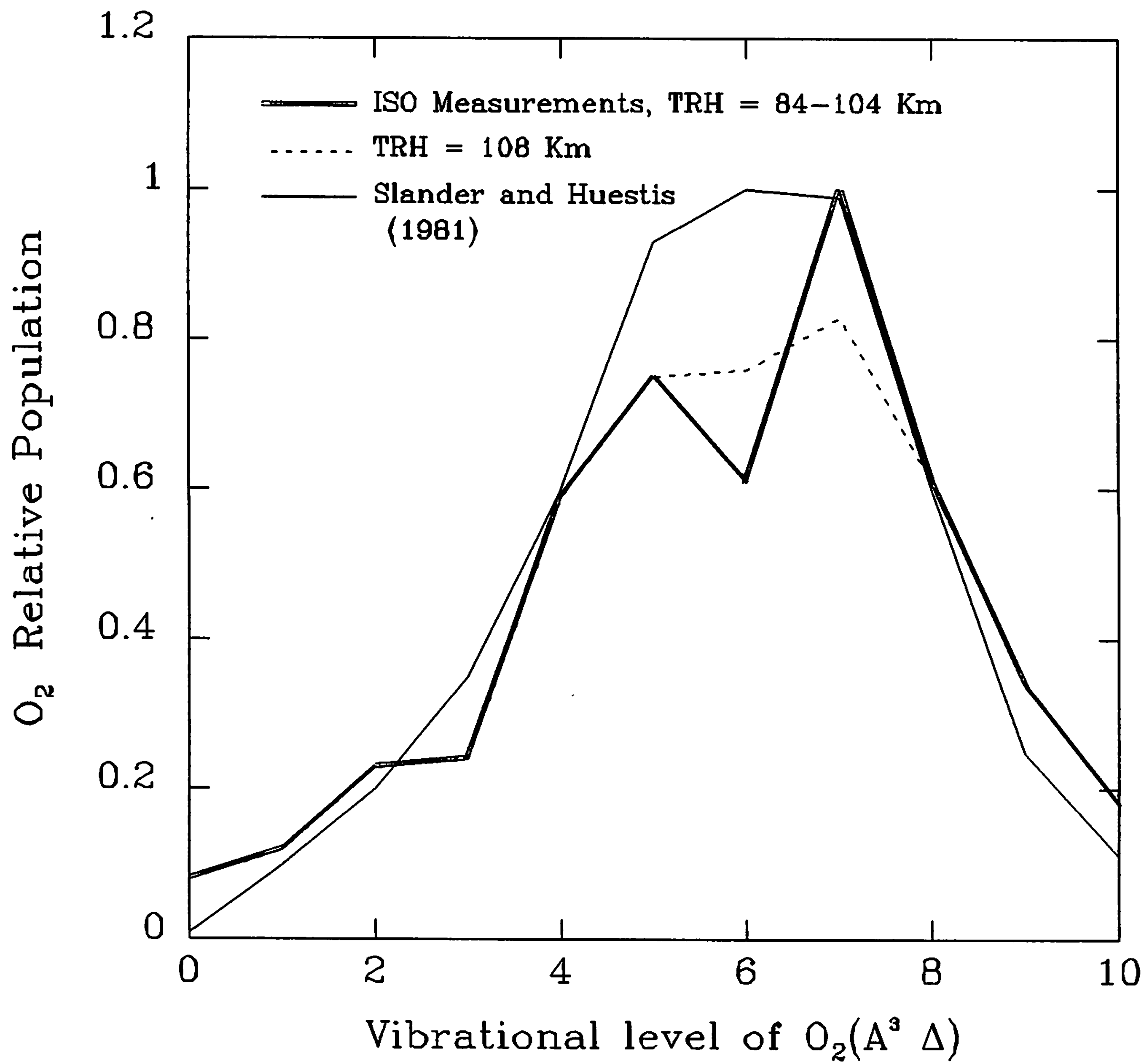

ISO Measurements, TRH = 84-104 Km
TRH = 108 Km
Slander and Huestis
(1981)
1.2
1
0.8
0.6
0.4
0.2
0
0
2
4
6
8
10
$O_2$ Relative Population
Vibrational level of $O_2(A^3\ \Delta)$

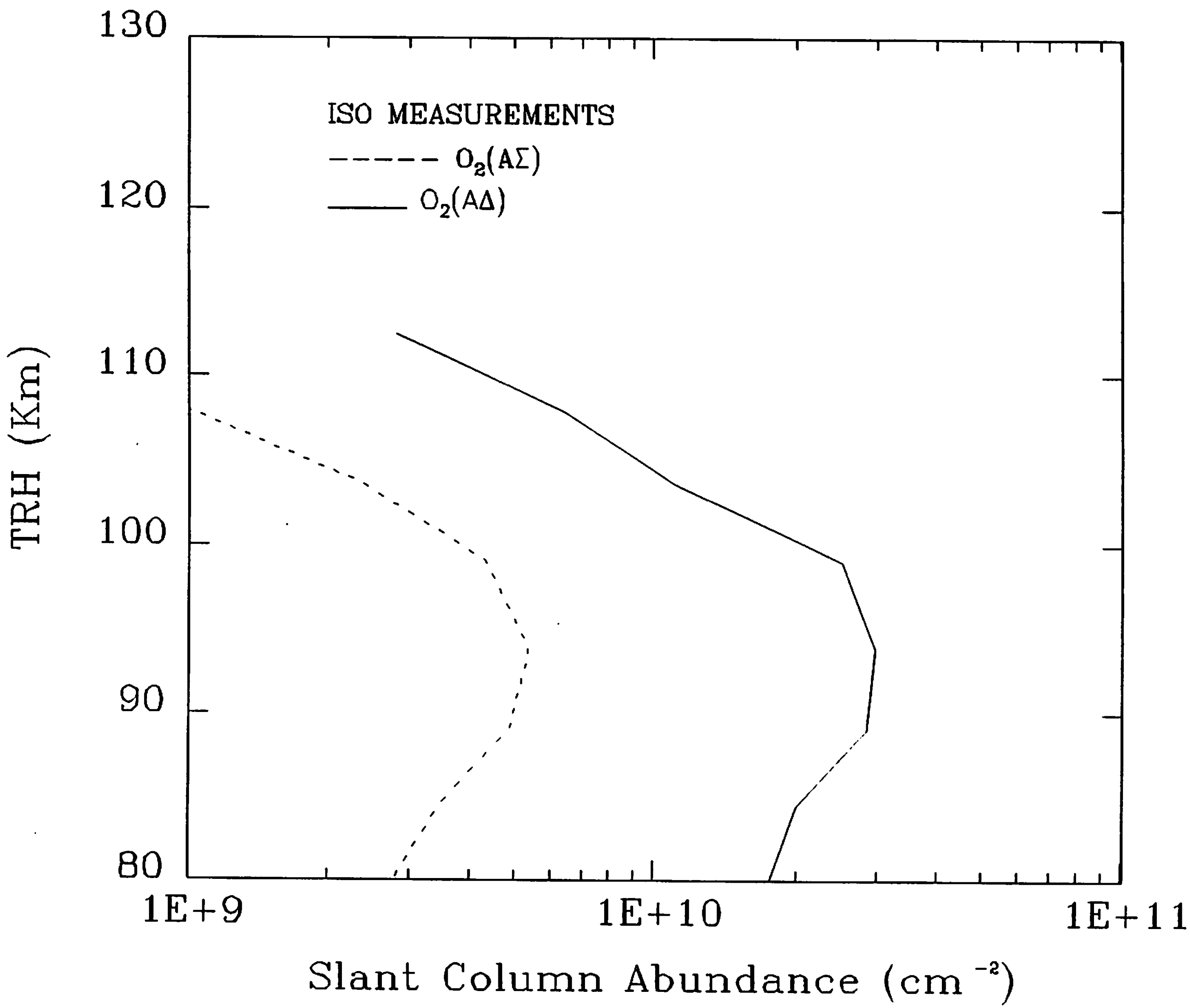

130
120
110
100
90
80
TRH (Km)
ISO MEASUREMENTS
O2(AΣ)
O2(AΔ)
1E+9
1E+10
1E+11
Slant Column Abundance (cm -2)

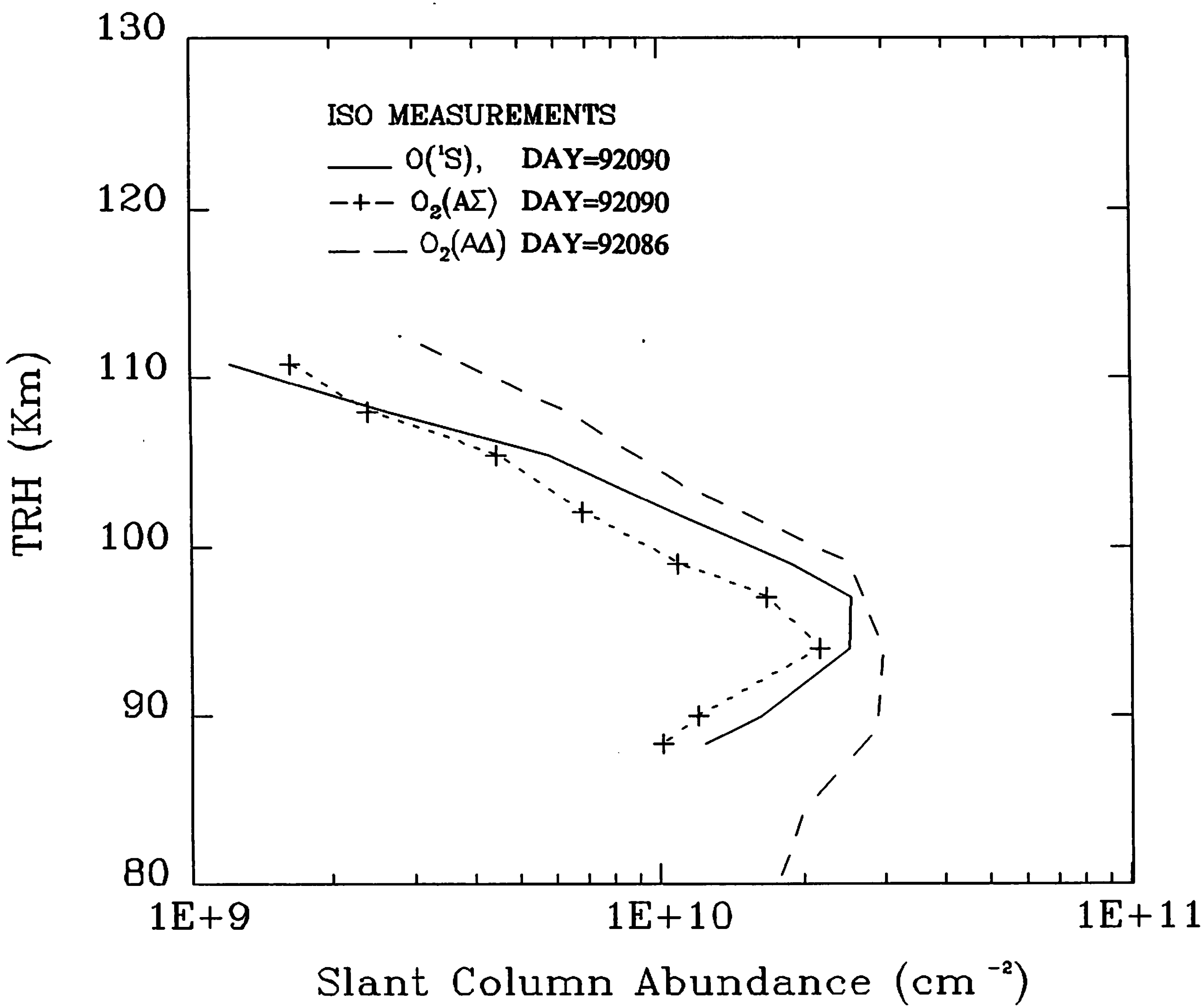

ISO MEASUREMENTS
O(¹S), DAY=92090
O₂(AΣ) DAY=92090
O₂(AΔ) DAY=92086
130
120
110
100
90
80
TRH (Km)
1E+9
1E+10
1E+11
Slant Column Abundance (cm⁻²)

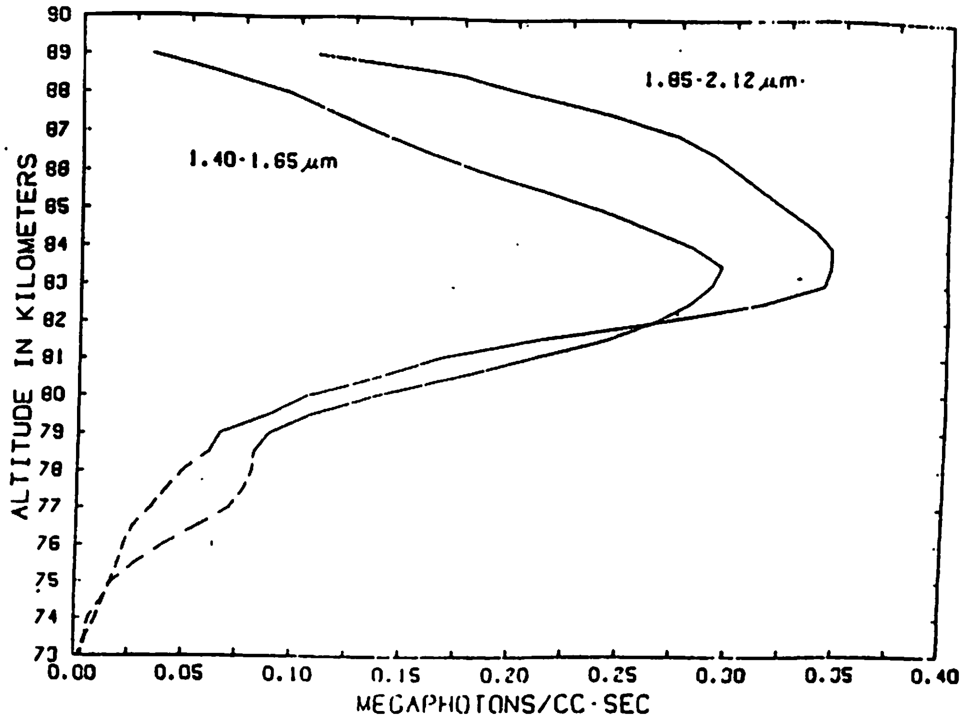


FIGURE 7A

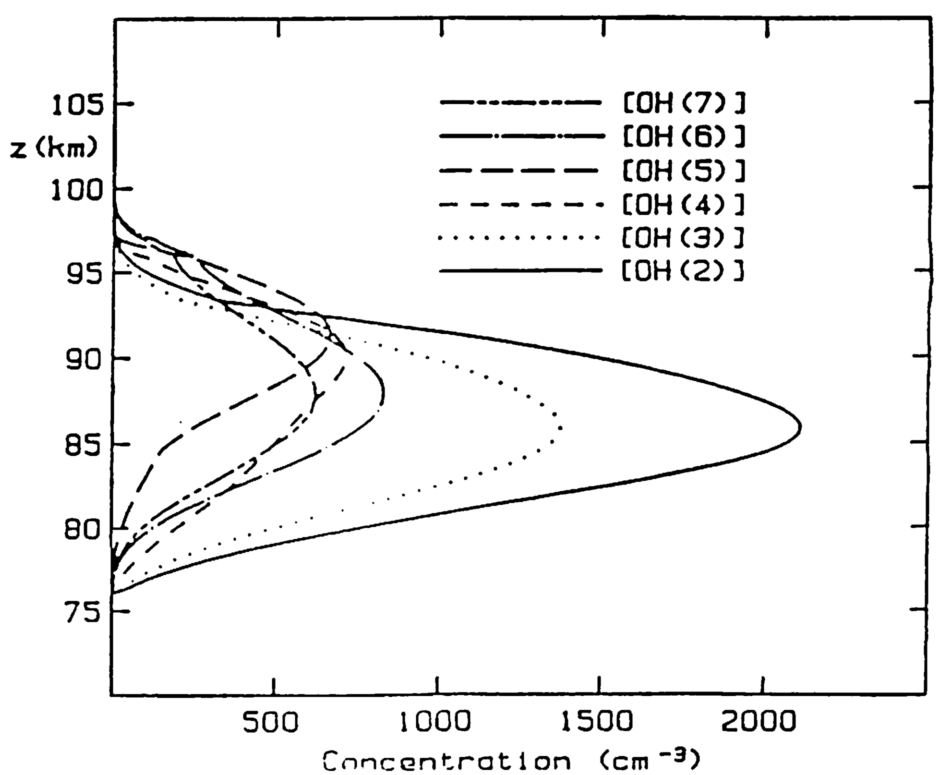


FIGURE 7B

# Metastable $O_2$ Daytime $O(^1S)$ Chemistry

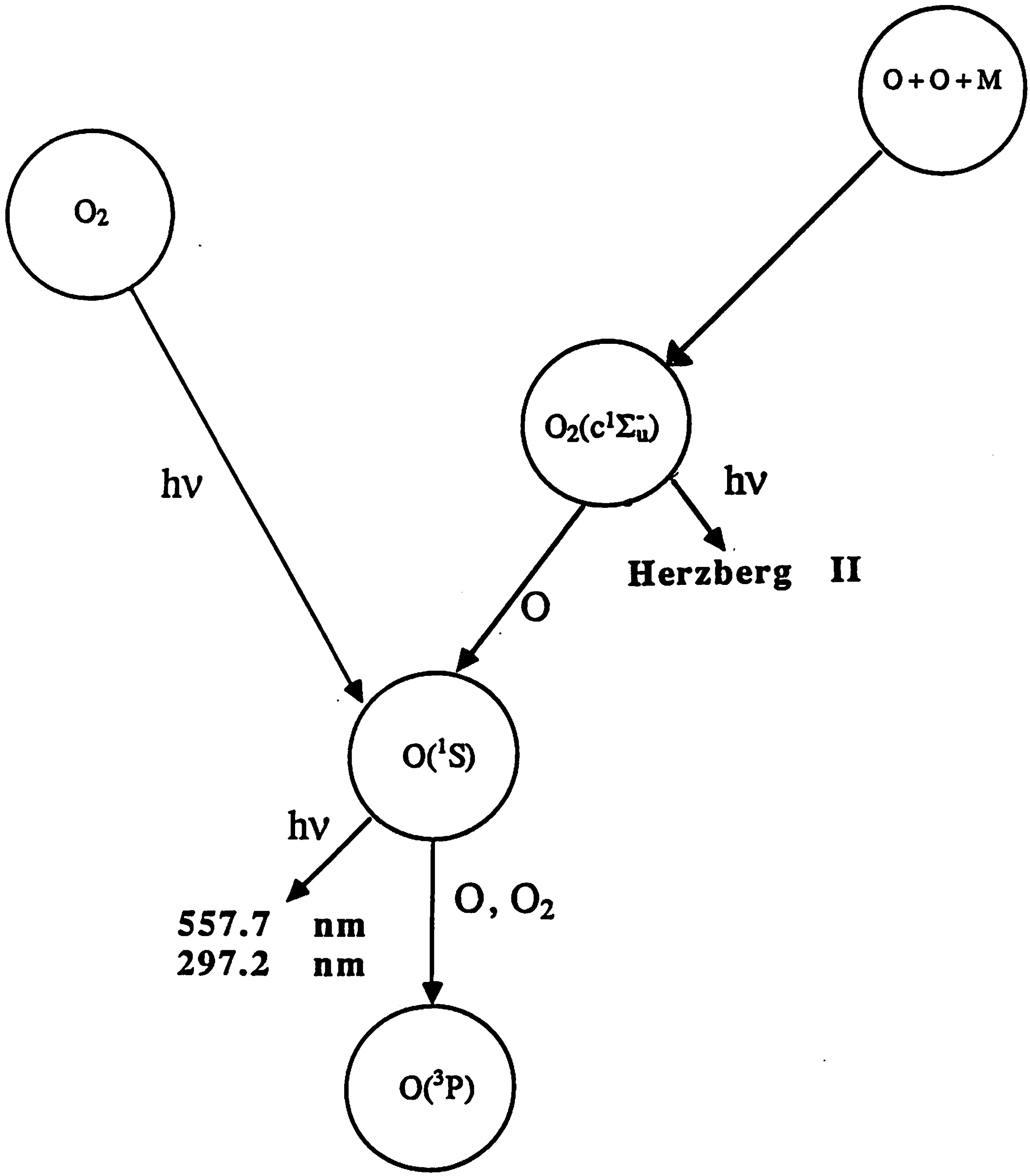

# DAYTIME $O_2$ ATMOSPHERIC BANDS

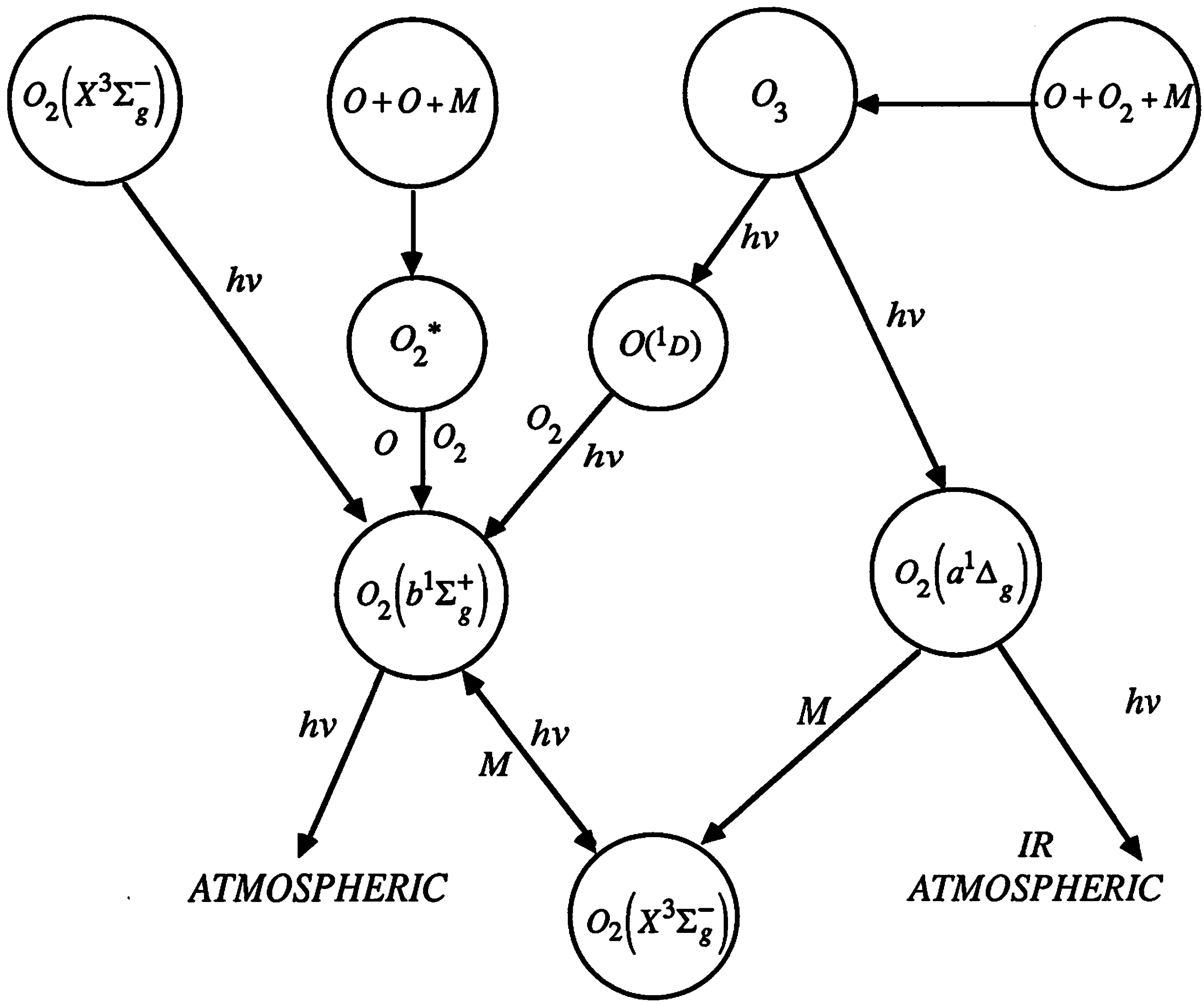

# PHOTOCHEMISTRY OF VIBRATIONALLY EXCITED HYDROXYL

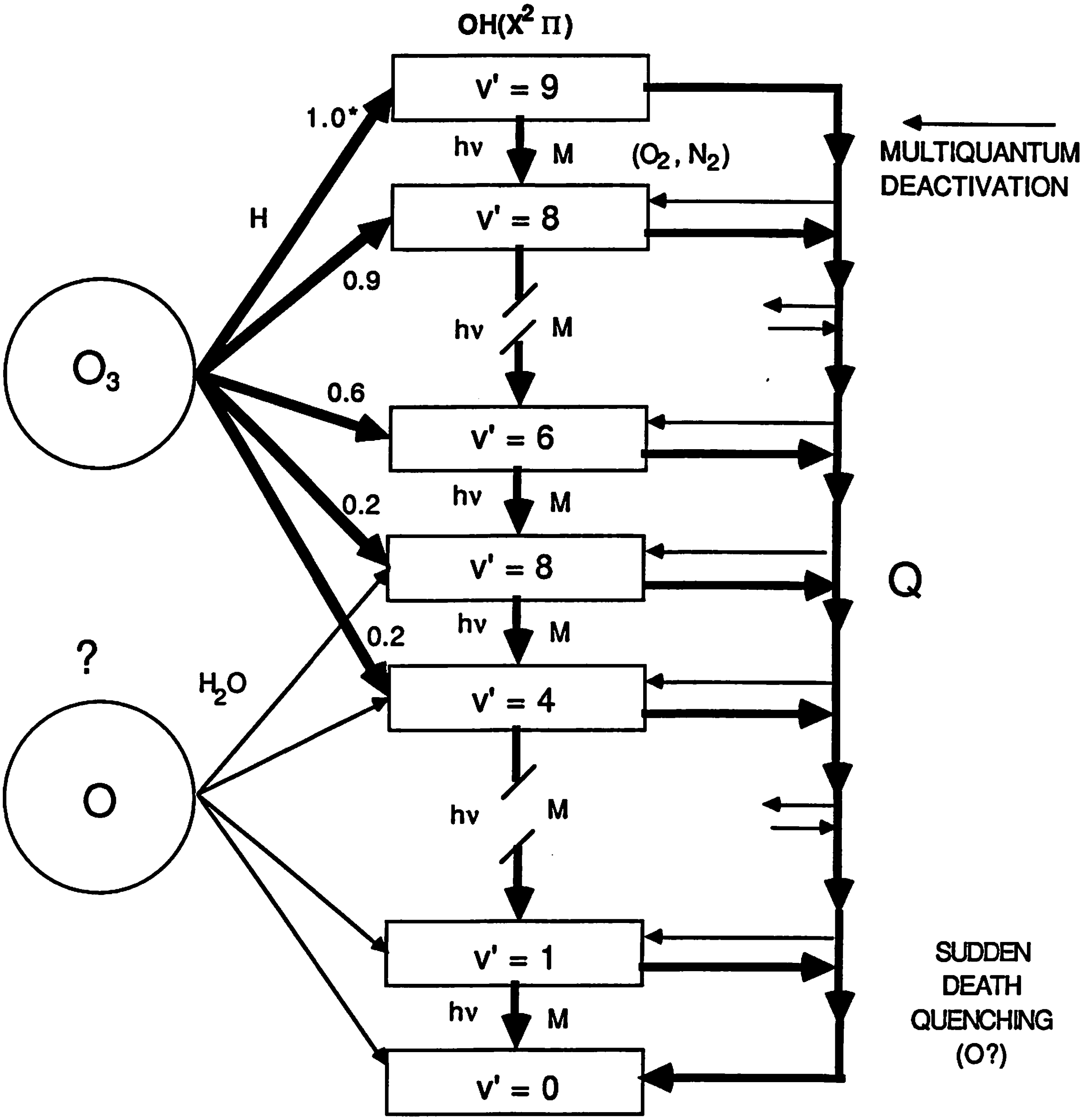


*BRANCHING RATIOS: McDade and Llewellyn (1987), Ohoyama et al. (1985)

**UNCERTAINTIES:**

1. WHETHER $HO_2 + O$ IS A SOURCE.
2. COLLISIONAL DEACTIVATION RATE COEFFICIENTS.
3. ABSOLUTE TRANSITION PROBABILITIES
4. PRODUCTS OF COLLISIONAL DEACTIVATION AS A FUNCTION OF SPECIES.

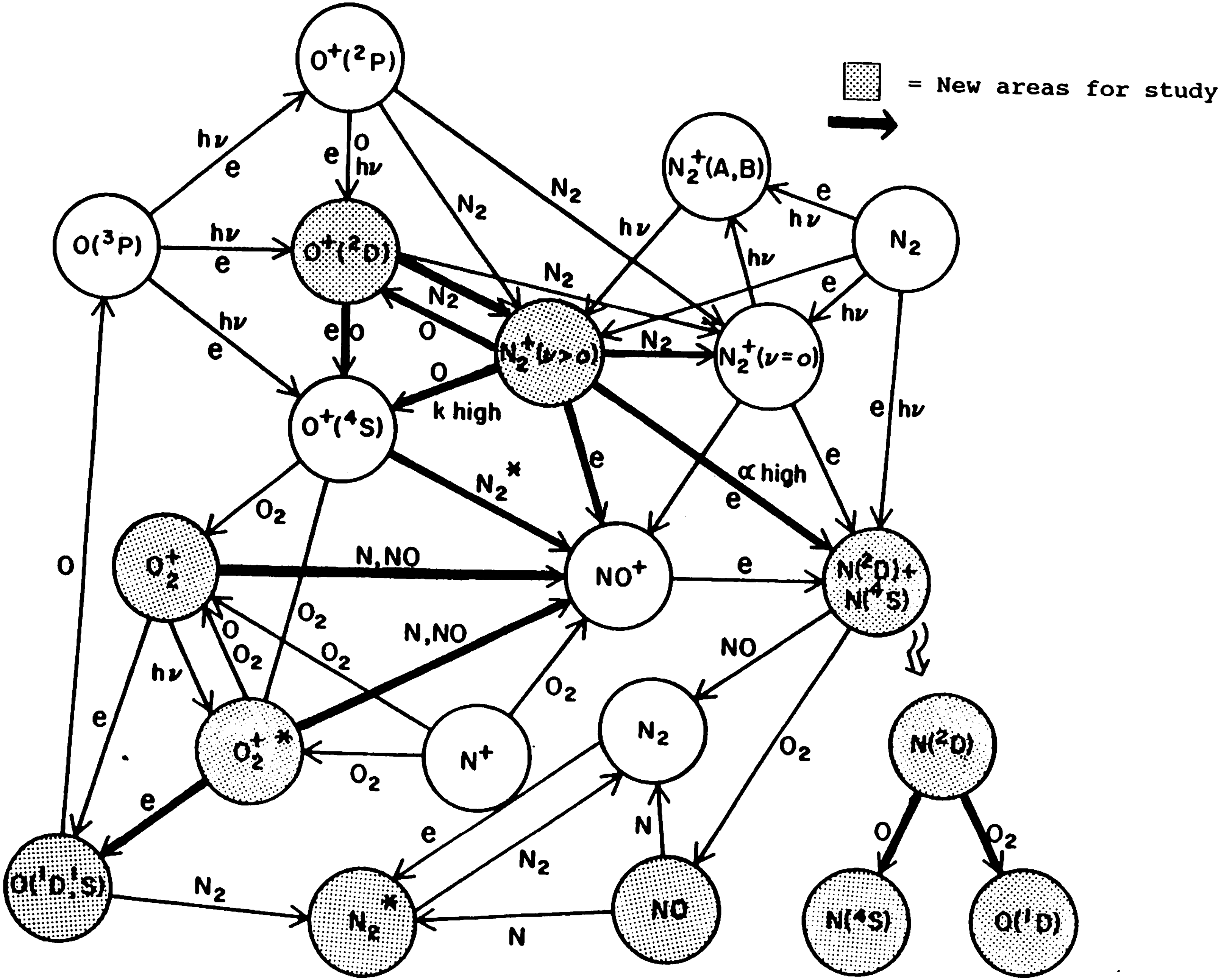


Schematic of the thermospheric and ionospheric chemistry to be studied

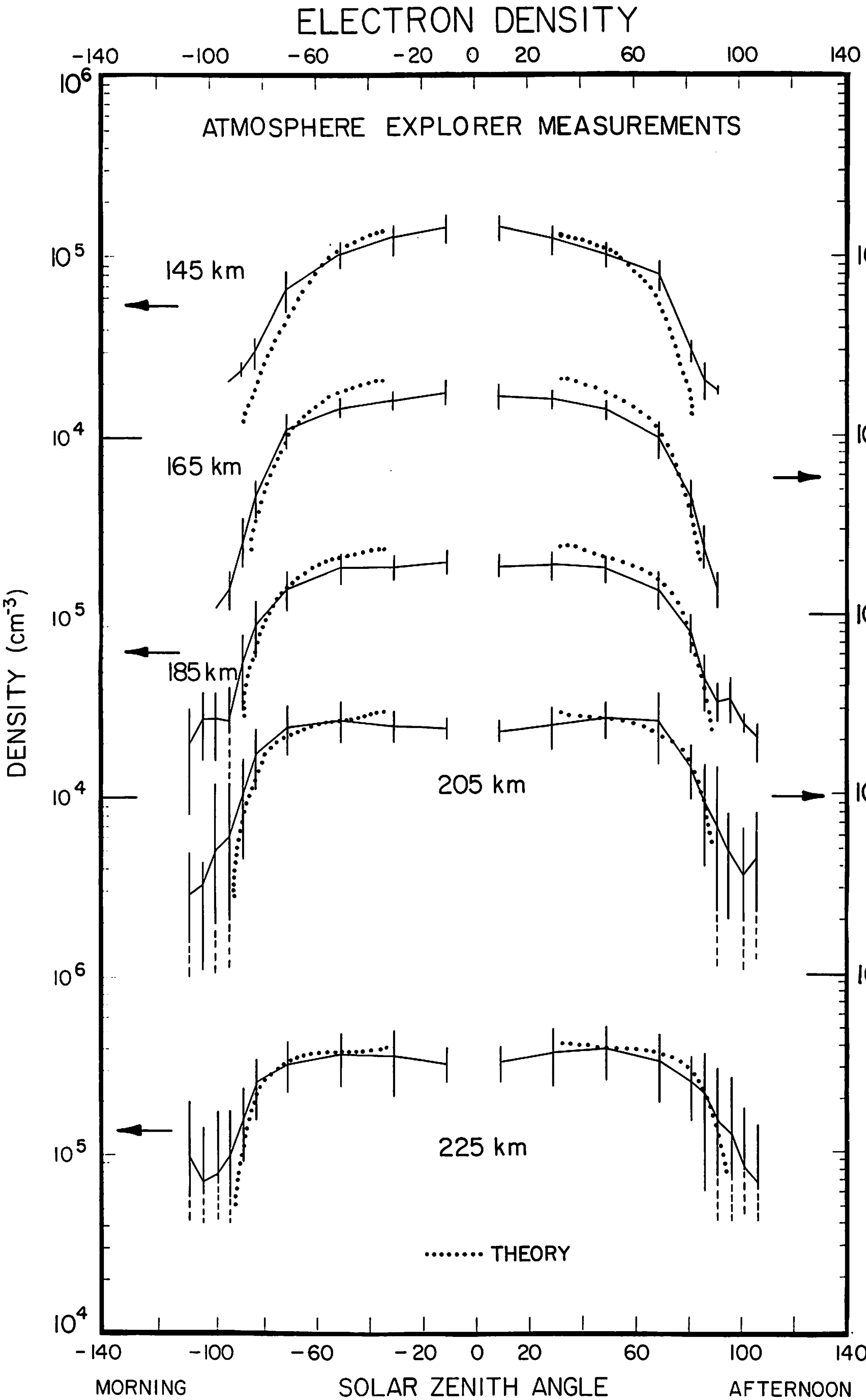

ELECTRON DENSITY
ATMOSPHERE EXPLORER MEASUREMENTS
145 km
165 km
185 km
205 km
225 km
THEORY
DENSITY (cm⁻³)
-140 -100 -60 -20 0 20 60 100 140
MORNING
SOLAR ZENITH ANGLE
AFTERNOON

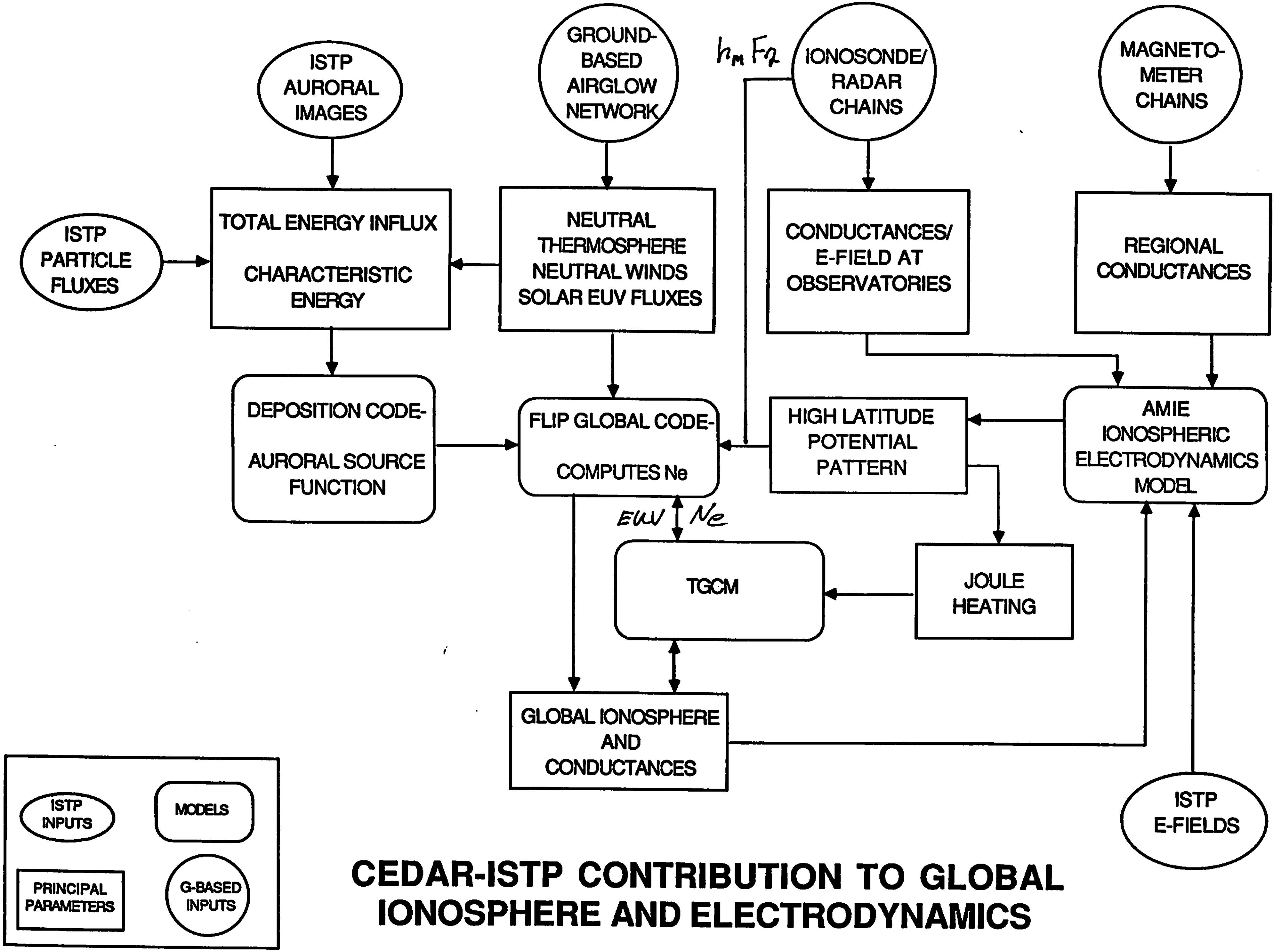


**CEDAR-ISTP CONTRIBUTION TO GLOBAL IONOSPHERE AND ELECTRODYNAMICS**